GENERAL INTRODUCTION

Biological aerated filters (BAFs) are wastewater treatment units that are capable of providing carbon oxidation, nitrification, and denitrification (Stensel et al., 1988; Pujol et al., 1994; Rogalla et al., 1990; Peladan et al., 1996). As high-rate, attached growth systems, they employ submerged media to support biomass and filter suspended solids. Densely populated active biomass then become attached to and entrapped in a porous support media. The process enables compact treatment due to the dense biomass and elimination of the need for secondary clarification. Without clarification, BAFs can be operated independent of sludge settling parameters that frequently limit the design and operation of conventional activated sludge systems. Full-scale BAF systems are capable of processing high pollutant and/or hydraulic loadings and are suitable for plant upgrades, expansions, water reuse, and various industrial processes.

Despite the advantages, aeration of any aerobic biological system consumes most of the power required for the process. Therefore, optimizing aeration capacity and efficiency can significantly influence the overall process economics (Mendoza-Espinosa and Stephenson, 1999). Yet hurdles lie in determining accurate oxygen transfer capabilities of a BAF unit. Although many methods are available to measure the rate of oxygen transfer in wastewater, the accuracy of several experimental procedures has been questioned (Capela et al., 1999) and data collection and analysis methods continue to be debated (Ruchti et al, 1985; ASCE, 1997; Brown and Balliod, 1982). Reliable methods of measuring oxygen transfer under process conditions and the variability of scaling up data from bench-scale units are still points of contention. In addition, the BAF itself remains somewhat of a black box process. The biomass and its mechanistic influence in a fixed-film process environment are not fully comprehended. Although published micro and macro-scale models incorporate key interaction parameters explaining the overall microbial behavior, researchers have made simplifying assumptions on even some of the most fundamental aspects of the system (Jacob et al., 1997; LeTallec et al., 1999; Mann and Stephenson, 1997; Poughon et al., 1999; Rittmann and Manem, 1992; San et al., 1993; Saez and Rittmann, 1988).

Mass-transfer characteristics of BAFs are influenced by numerous factors including the superficial gas and liquid velocities, temperature, media porosity and size, filter depth, suspended solids concentration, wastewater to clean water characteristics, gas holdup, bulk dissolved oxygen (DO) concentrations, and diffusion kinetics (Alexander and Shah, 1976; Danill and Gulliver, 1988; Kent et al., 2000; Moore et al., 2001; Mendoza-Espinosa and Stephenson, 1999). A recent review concluded that, in particular, the biofilm in a BAF has a significant positive effect on oxygen transfer efficiency which suggests the possibility for biological oxygen transfer enhancement (BOTE) (Mendoza-Espinosa and Stephenson, 1999). The presence of BOTE has been suggested in activated sludge, rotating biological contactors, and fermentation processes with many researchers agreeing to the presence of a separate oxygen transfer mechanism in biological systems that cannot be accounted for in traditional diffusion kinetics (Albertson and DiGregorio, 1975; Tsao, 1968; Ju and Sundararajan, 1992; Mines and Sherrad, 1985; Lee and Stensel, 1986; Harris et al., 1996; Sundararajan and Ju, 1995; Reiber and Stensel, 1985).

In other BAF systems, an overall rate of oxygen transfer 1.2 to 3.2 times above the rate that would be expected for diffused aeration alone was determined with the presence of a biologically active biofilm (Harris et al., 1996; Lee and Stensel, 1986; Reiber and Stensel, 1985). The studies of the BAF systems also found increasing enhancement factors corresponding to increases with the biomass concentration, pollutant removal load and available interfacial surface area. The presence of the media bed has been shown to minimize bubble coalescence as well as to increase the gas retention time within the bed (Fuije et al., 1992). Yet some researchers also question the existence of oxygen transfer enhancement. The enhancement phenomenon observed in biological systems does not coincide with the traditional retardation in oxygen transfer factors when comparing wastewater to clean water (Iranpour et al., 2000; Pelkonen, 1990). In addition, oxygen transfer determinations can vary significantly based on process conditions and between in-situ sampling and ex-situ analysis of samples (Mueller and Stensel, 1990). Still others determined that the traditional kinetics can account for oxygen transfer even in the presence of biomass (Nogueira et al., 1998; Vaxelaire et al., 1995)

Although a number of researchers have attempted to study the substantial potential enhancement in the oxygen transfer rate in biological processes, the actual transfer mechanism limitations are still not well understood. The objective of this research was to 1) evaluate oxygen transfer kinetics under conditions without biological growth by the development of a predictive relationship of major contributing factors, 2) investigate the oxygen transfer capabilities of a tertiary BAF unit with high oxygen demand requirements through a series of aeration process tests and 3) explore the presence of oxygen transfer enhancements calculated within the unit by further analyzing the actual transfer mechanism limitations. Collectively, the study is designed to evaluate the rates of supply and consumption of oxygen in BAFs.

MANUSCRIPT 1: MASS-TRANSFER CHARACTERISTICS OF A BIOLOGICAL AERATED FILTER

SUSANNA M. LEUNG*, JOHN C. LITTLE*, TROY HOLST** and NANCY G. LOVE*

*Department of Civil and Environmental Engineering, Virginia Polytechnic Institute and State University, Blacksburg, Virginia 24061-0246, USA

**Ondeo Degremont Inc., Richmond, Virginia 23229, USA

ABSTRACT – The mass-transfer characteristics of a submerged-media biological aerated filter have been determined over a wide range of gas and liquid flow rates. The mass-transfer coefficients ($K_La_{(T)}$) were measured using a nitrogen gas stripping method and were found to increase as both gas and liquid superficial velocities increase, with values ranging from approximately 40 to 380 h^{-1}. The effect of parameters including the gas and liquid velocities, dirty water to clean water ratio, and temperature dependence was successfully correlated within $\pm$ 20% of the experimental K_La value. The effects of the media size and gas holdup fractions were also investigated. Stagnant gas holdup did not significantly influence the rate of oxygen transfer. Dynamic gas holdup and the difference between total and stagnant gas holdup were found to increase with an increase in gas velocity. Neither liquid velocity nor liquid temperature was determined to have a significant impact on gas holdup.

Key words – Alpha, Mass Transfer Correlation, BAF, Gas Holdup, Oxygen, Theta

NOMENCLATURE

a =	empirical factor of U_G for the predicted K_La determination
b =	empirical factor of U_L for the predicted K_La determination
c =	overall empirical factor for the predicted K_La determination
C	bulk oxygen concentration (mg/L)
C_{avg}	linear average between maximum and minimum bulk DO concentration (mg/L)
C_{in}	bulk oxygen concentration in the reactor influent (mg/L)
C_{out}	bulk oxygen concentration in the reactor effluent (mg/L)
C_{sat}	liquid phase saturated O_2 concentration at gas-liquid interface (mg/L)

H	depth of water in the column (m)
H_I	height of water in column with no gas bubbles present (cm)
H_S	height of water in column with the presence of stagnant gas holdup (cm)
H_T	height of water in column with the presence of total gas holdup (cm)
H_{water}	height of the water column (cm)
J_{O2}	maximum reaeration oxygen flux (mg/L/h)
$K_La_{(T)}$	mass transfer coefficient based on void or liquid volume at temperature T (h^{-1})
m	Henry's law constant
P	100,000 Pa/bar
P_t	total hydrostatic pressure (bar)
T	temperature (degree Celsius)
U_G	empty bed superficial gas velocity at normal conditions of 1 atm and 20^{o}C (Nm/h)
U_{IL}	interstitial liquid velocity (m/h)
U_L	empty bed superficial liquid velocity (m/h)
V_L	volume of water in the column (L)
W_B	weight of water displaced by dynamic gas bubbles in the free water above bed (kg)
W_I	weight of the column with no gas bubbles present (kg)
W_S	weight of the column with the presence of stagnant gas holdup (kg)
W_T	weight of the column under process conditions –presence of total gas holdup (kg)
y	mole fraction of oxygen in the gas-phase
z	distance of water travel up the column (m)
α	$\frac{K_La_{wastewater}}{K_La_{clean\ water}}$ correction factor ratio
β	$\frac{DO_{sat\ wastewater}}{DO_{sat\ clean\ water}}$ correction factor ratio
ε	bed porosity
ε_{gt}	total gas holdup as a fraction of empty bed volume
ε_{gs}	stagnant gas holdup as a fraction of empty bed volume
θ	dimensionless constant for temperature correction

INTRODUCTION

Biological aerated filters (BAFs) are wastewater treatment units that are capable of providing carbon oxidation, nitrification, and denitrification (Stensel et al., 1988; Pujol et al., 1994; Rogalla et al., 1990; Peladan et al., 1996). As high-rate, attached growth systems, they employ submerged media to support biomass and filter suspended solids. The process enables compact treatment due to the dense biomass and elimination of the need for secondary clarification. Without clarification, BAFs can be operated independent of sludge settling parameters that frequently limit the design and operation of conventional activated sludge systems. Full-scale BAF systems are capable of processing high pollutant and/or hydraulic loadings and are suitable for plant upgrades, expansions, water reuse, and various industrial processes. Aeration of the BAF consumes most of the power required for the process. Therefore, optimizing aeration capacity and efficiency can significantly influence the overall process economics (Mendoza-Espinosa and Stephenson, 1999). Although many have studied oxygen transfer in aeration tanks, few have examined diffused-bubble aeration in BAFs.

The mass-transfer characteristics of BAFs are influenced by the superficial gas and liquid velocities, temperature, media porosity and size, filter depth, suspended solids concentration, wastewater to clean water characteristics, and gas holdup (Alexander and Shah, 1976; Danill and Gulliver, 1988; Kent et al., 2000; Moore et al., 2001; Mendoza-Espinosa and Stephenson, 1999). Many methods are available to measure the rate of oxygen transfer in wastewater, including sulfite oxidation, inert gas tracer exchange, off-gas analysis, and liquid super-saturation (Alexander and Shah, 1976; Goto et al., 1991; Iranpour et al., 2000; Linek and Vacek, 1981). Yet, the accuracy of several experimental procedures has been questioned (Capela et al., 1999) and data collection and analysis methods continue to be debated (Ruchti et al, 1985; ASCE, 1997; Brown and Balliod, 1982).

The objective of this research was to develop a predictive relationship for the gas-liquid mass-transfer coefficient in an upflow BAF. The effect of media type, hydraulic loading rate, air loading rate, temperature, and gas holdup on the mass-transfer coefficient was evaluated. This paper will focus on evaluating oxygen transfer kinetics under conditions

without biological growth. The influence of biological growth on the rate of oxygen transfer is described in a subsequent paper (Leung et al., 2003). Collectively, these papers evaluate the rates of supply and consumption of oxygen in BAFs. Ultimately, this information will be used to optimize overall system performance.

MASS TRANSFER THEORY

The oxygen transfer capability of the BAF unit was tested using an inert gas stripping method. Pure nitrogen gas was bubbled into oxygen saturated water at the base of the BAF unit. As both gas and water traveled up the column, two kinetic processes simultaneously, yet independently, took place where 1) dissolved oxygen transferred from the liquid phase to the gas phase and 2) nitrogen gas dissolved into the liquid phase. Both processes were driven by their respective kinetic rates to reach a state of equilibrium. The rate of oxygen dissolution could then be measured by plotting the decreasing concentration of dissolved oxygen as the water traveled up the column.

Dissolved oxygen profile analysis

To simplify the determination of the oxygen mass-transfer coefficient in the packed media bed, it was assumed that water passes up through the un-fluidized media in plug-flow, the pH, porosity, temperature, and initial dissolved oxygen (DO) remain constant during operation, and the entire system was at steady-state. A mass balance of dissolved oxygen in the water then yields:

$$\frac{dC}{dz} = \frac{K_L a\,(\varepsilon - \varepsilon_{gt})}{U_L}\left(C_{sat} - C\right) \qquad (1.1)$$

where K_La is the mass transfer coefficient based on the liquid volume. The saturated aqueous oxygen concentration at any depth is given by (Little, 1995):

$$C_{sat} = \frac{y\,P_t}{m} \qquad (1.2)$$

Oxygen transfer tests were conducted using a bench-scale column to measure the oxygen transfer rates under rigorously controlled conditions. Under the testing setup, the

accumulation of oxygen in the nitrogen gas is small, allowing C_{sat} to remain essentially zero (y = 0). The hydrostatic pressure within the column is close to atmospheric conditions because of the relatively shallow water depth. With these simplifications, the dissolved oxygen concentration profile becomes exponential with column height, or:

$$C_{out} = C_{in} \cdot \exp\left(-\frac{\left(\varepsilon - \varepsilon_{gt}\right)(K_L a)(z)}{U_L} \right) \tag{1.3}$$

Microsoft Excel XP's Solver program was then used to provide a least-squares fit of the measured oxygen concentration profile to Equation 1.3 to determine the K_La factor. The mass transfer coefficient can also be based on the void volume or porosity (which is constant) rather than liquid volume (which changes as gas holdup changes) and this is achieved by setting ε_{gt} to zero in Equation 1.3. In this paper, K_La values will be based on void volume unless otherwise indicated.

Temperature correction factor (θ) and K_La correlation

K_La can be expressed as a function of temperature by fitting the data using SigmaPlot 8.0 and the following well-established equation:

$$K_L a_{(T)} = K_L a_{(20)} \times \theta^{(T-20)} \tag{1.4}$$

SigmaPlot 8.0 uses the Marquardt-Levenberg algorithm to fit a representative curve to the data (SPSS Science, Chicago, IL). Past studies have reported θ values ranging from 1.008 to 1.047, although the value of 1.024 is common and has a firm theoretical foundation (Danill and Gulliver, 1988). Using the temperature normalized $K_La_{(20)}$ data, individual non-linear regressions that correlate K_La with superficial gas and liquid velocities were determined for each clean water test condition assuming the following relationship using SigmaPlot 8.0 (Alexander and Shah, 1976):

$$K_L a_{(20)} = (c) \cdot U_G^a \cdot U_L^b \tag{1.5}$$

"Dirty" water to clean water ratios

The mass transfer characteristics are further influenced by the constituents of the liquid phase. The ratio between the oxygen transfer coefficient found in wastewater and clean water is commonly referred to as alpha (α). The alpha factor for a particular wastewater is dependent on many chemical and process parameters. These include COD, surface tension, liquid temperature, the presence of suspended solids, reactor dynamics and aeration methods and velocities (Pelkonen, 1990). The ratio between the wastewater and clean water oxygen saturation concentrations is commonly referred to as beta (β). The beta factor is dependent on the overall effect of dissolved gases, organics, salts, liquid temperature, and pressure (Tchobanoglous et al., 2003). Studies on activated sludge processes have shown that alpha values can vary significantly, depending on the degree of treatment the wastewater has received (Pelkonen, 1990; Groves et al., 1992). Pelkonen (1990) found that alpha at a particular wastewater treatment plant doubled between the primary effluent and the secondary effluent. Alpha factors have been found to vary from 0.3 to 0.9 within an aeration basin (Iranpour et al., 2000; Pelkonen, 1990). Harris et al. (1994) found alpha factors between 0.8 and 1.6 for a downflow BAF. Such variations introduce significant variability when comparing rates of oxygen transfer in clean water and wastewater. The DO saturation factor between wastewater and clean water has previously been found to be close to 1 in a BAF treating municipal wastewater (Reiber and Stensel, 1985; Harris et al., 1994). A beta value of 1 was assumed to apply in this study.

EXPERIMENTAL METHODS

A ten-centimeter diameter bench-scale upflow biological aerated filter column was fabricated and used to evaluate the oxygen transfer characteristics of two types of clay media and associated support gravel. The overall column was approximately 1.3 m in height with liquid sampling ports located at regularly spaced 5.1 cm intervals. The gravel and media height within the column were adjusted according to the material tested (see Table 1.1). The bench-scale column was fabricated from two sections of clear acrylic pipe, separated by a flange to allow for the insertion of a water nozzle plate. The bottom section of the column served as a

reservoir for the inlet water, and provided uniform water distribution through the nozzle into the section above. The top section of the column housed two gravel support layers underneath a clay media bed. The support gravel protected the water inlet nozzle from being clogged by clay media and improved distribution of gas bubbles across the surface area of the column. The inlet water was pumped from a reservoir by a Cole Palmer MasterFlex Model 7553-70 peristaltic pump (Vernon Hills, IL), through a constant temperature bath (24°C clean water testing only), and into the bottom of the column as shown in Figure 1.1.

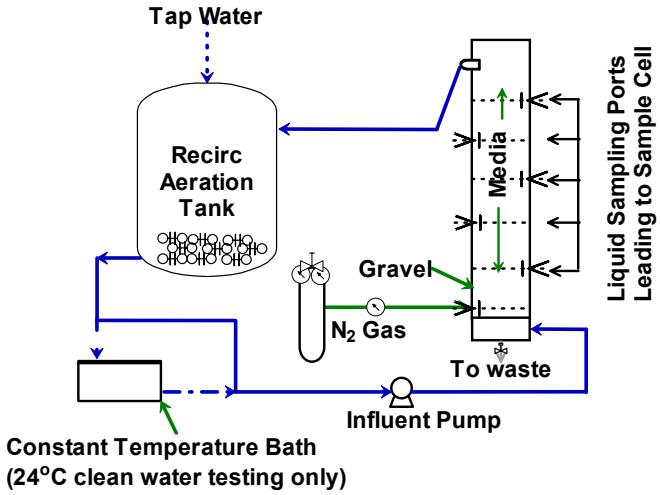

Figure 1.1: Bench-scale column schematic

Two types of clay media were tested. Both sizes were manufactured from a thermally-expanded clay material. One was an angular shaped clay media crushed to an effective size of 2.7 mm. The other was a spherical shaped clay media crushed to an effective size of 3.5 mm. Two types of support gravel (I and II) were also tested with nominal diameters between 2 and 2.5 cm and between 1 and 2 cm, respectively.

Table 1.1: Bench-scale column characteristics

	Gravel Testing	**Media Testing**
Overall Height	1.3 m	1.3 m
Media Height	21 cm	35 cm
Type II Gravel Height	15 cm	None
Type I Gravel Height above Air Inlet	22 cm	15 cm
Height of free water	10 cm	10 cm
Gas flow rate capacity	0 – 8 std L/min	0 – 8 std L/min
Water flow rate capacity	0 – 4 L/min	0 – 4 L/min
Water Temperature	9 – 25 °C	9 – 25 °C

Dissolved oxygen concentration profile

Transfer of dissolved oxygen into nitrogen gas passing up through the column created a dissolved oxygen concentration profile at steady-state. Sampling tubes were installed along the height of the reactor for liquid withdrawal. Each sampling tube consisted of a single 6 mm external diameter horizontal SCH80 PVC pipe which spanned the diameter of the column. Disruption of upward flow in the column by the sampling tubes was minimized by alternating the connectors at 0 and 90 degree positions across the circumference of the column. The sampling tubes were threaded to the connector at one end and capped at the other end. Water was drawn into the sample pipe through a 1.6 mm diameter bored hole facing upwards in the center of the column. Gas bubbles were prevented from entering the sample tube by a cone-shaped deflector surrounding the inlet hole.

Holox Ultra Pure >99.998% nitrogen gas (Norcross, GA) was supplied to the column through a 1.6 mm diameter bored hole facing downwards in the center of the injection pipe. With the exception of the orientation of the bored hole, the gas injection tube was identical to the DO sampling tube. A Gilmont Instruments Model 150 mm flowmeter (Barrington, IL) allowed precise manual control of the flow rate of nitrogen gas entering the column.

Sampling of the dissolved oxygen concentration profile commenced after the system reached steady-state. Minimal disruption was achieved by first extracting samples at the topmost port and then continuing consecutively down the column. Representative water samples were extracted through 6 mm internal diameter vinyl tubing to a 60 mL custom designed, magnetically-stirred, flow-through sample cell at controlled flow rates of 60-120 mL per minute. The length of vinyl tubing introduced a 15 to 30 second sample delay. A YSI Model 5100 meter and Model 5470 field probe (Yellow Springs, OH) recorded dissolved oxygen concentrations using a high-sensitivity membrane for clean water tests and a standard membrane for dirty water tests after a minimum of 3 liquid volumes had flushed the cell and a stable reading was obtained (approximately 5 to 10 minutes). The water in the cell was completely mixed and sealed from any air-water transfer by a dissolved oxygen probe gasket

fitting. During the dirty water testing, the stability of the dissolved oxygen concentration in the inlet water was monitored using a second DO probe (YSI Model 55).

Municipal drinking water (tap) served as the clean water source while domestic secondary effluent from two local wastewater treatment plants served as the source of dirty water. Between dirty water testing runs, water flow was stopped and the media bed was dosed with concentrated hypochlorite dosages every 4 hours to prevent significant biological activity interferences. The system was then flushed for approximately 10 minutes with secondary effluent (which was sent to waste) to eliminate the presence of chlorine within the column and to minimize the addition of chlorine to the recirculated water before hydraulic loading resumed. The water quality constituents of interest were analyzed over the course of the experiments on a daily basis for the 24^{o}C testing and on a weekly basis for the 10^{o}C testing. Alkalinity samples were analyzed immediately according to Standard Methods 2320B (APHA, 1998). Ammonium-nitrogen samples (100 mL) were preserved and analyzed using Standard Methods 4500-NH3C. Nitrite and nitrate samples were filtered (Whatman 0.45 μm), frozen, and analyzed using a DIONOX Model DX-120 (Sunnyvale, CA) ion chromatography (Standard Methods 4500-NO_2^-C and 4500-NO_3^-C). Chromeleon analysis software was used to quantify chromatograms. COD and DOC values were measured using Standard Methods 5220C and 5310C, respectively. COD samples were preserved with concentrated sulfuric acid at a pH of less than 2 and refrigerated until analyzed (within 28 days). DOC samples were filtered (Whatman 0.45 μm), acidified with 85% phosphoric acid, and frozen until analyzed. Analysis was performed using a Sievers 800 Portable Total Organic Carbon Analyzer and Sievers Instruments TOC Autosampler Program V.3.14 analysis software. All nitrogen species analysis was performed in duplicate; all other analyses were performed in triplicate.

Mass transfer tests in clean water were performed for the 2.7 media, and gravel layers at liquid temperatures of 10, 16, and 24 $\pm$ 1 ^{o}C for the matrix of nominal superficial air and water velocities shown in Table 1.2. Additional clean water testing was carried out for the 3.5 mm media, but only at a liquid temperature of 10 $\pm$ 1^{o}C. For the experiments at 10 and 16^{o}C, recirculated water in a constant temperature room was used to control the temperature

of the liquid. The experiments at 24°C were performed in a 20°C environment with continuous "fresh" source water drawn from the laboratory tap and heated using a constant temperature bath. Between each test condition, the column was drained and flushed with water a minimum of 3 times to dispel any stagnant bubbles remaining from the previous test. The test matrix was performed in duplicate for the 2.7 and 3.5 mm media, with single experiments for the gravel layers.

Table 1.2: Oxygen transfer testing matrix with superficial velocities based on empty bed volume. D_{16} = dirty water aeration testing for gravel at 16°C; D_{24} = dirty water aeration testing for 2.7 mm media at 24°C; C_T = aeration testing for all other temperatures and liquids not specifically stated.

	Superficial Liquid Velocity (m/h)				
Superficial Gas Velocity (Nm/h)		***4***	***8***	***12***	***16***
	8	C_T, D_{16},	C_T, D_{16},	C_T, D_{16}, D_{24}	C_T, D_{24}
	16	C_T, D_{16},	C_T, D_{16},	C_T, D_{16}, D_{24}	C_T, D_{24}
	24	C_T, D_{16},	C_T, D_{16},	C_T, D_{16}, D_{24}	C_T, D_{24}
	32	C_T	C_T, D_{16},	C_T, D_{16}, D_{24}	C_T, D_{24}
	40	C_T	C_T	C_T, D_{16}, D_{24}	C_T, D_{24}

Dirty water oxygen transfer tests were conducted for the 2.7 mm and 3.5 mm media at liquid temperatures of 10 $\pm$ 1 °C for the full matrix shown in Table 1.2. In addition, the 2.7 mm media, the gravel layers were tested at 16 and 24 $\pm$ 1 °C using the abbreviated matrix shown in Table 1.2. Dirty water oxygen transfer tests were performed in a temperature controlled room with secondary effluent from one local POTW for the 10°C test and at a separate local POTW for the higher temperature tests. Both sources of secondary effluent were primarily domestic in nature.

Gas holdup

Gas holdup can significantly influence oxygen transfer within a packed bed (Ohshima et al., 1976, Fujie et al., 1992). Gas holdup within the 2.7 mm and 3.5 mm media beds was therefore determined in conjunction with the series of oxygen transfer experiments. Volumetric and gravimetric methods were used to determine both stagnant and dynamic gas holdup.

In the volumetric method, the column was flushed of gas bubbles and filled in an upflow fashion to a water level approximately 1 cm above the level of the media. Closing the liquid feed valve, the heights of the media and the water level in the column were individually marked. Nitrogen gas was then bubbled into the column until the height of the water stabilized (minimum 20 minutes). The gas feed valve was closed and the dynamic gas bubbles allowed to discharge from the column. Water height was recorded after stabilization of the column. Gas holdup was determined in triplicate for the 2.7 mm media in clean water at liquid temperatures of 16°C and 24°C, for superficial gas velocities of 8, 16, 24, 32, and 40 Nm/h, respectively using the following equations:

$$\varepsilon_{gt} = \frac{H_T - H_I}{H_{water}} \tag{1.6}$$

$$\varepsilon_{gs} = \frac{H_S - H_I}{H_{water}} \tag{1.7}$$

The gravimetric method enables measurement of gas holdup under flowing water conditions. The column was placed on an Ohaus Ranger RD30LS electronic balance (Pine Brook, NJ) and flushed of gas bubbles. An initial stable weight was recorded. The nitrogen gas feed was introduced and after the column stabilized (20-30 minutes) a second weight was recorded. The gas feed valve was closed and the final stabilized weight was recorded with the stagnant bubbles remaining in the bed. The tests for the 2.7 mm media were each performed in duplicate at liquid temperatures of 10 and 16°C for clean water and 10 and 24°C for dirty water for the full gas/liquid testing matrix outlined in Table 1.2. The results were used to determine total, dynamic, and stagnant gas holdup fractions as a function of gas flow rate using the following equations:

$$\varepsilon_{gt} = \frac{W_I - W_T - W_B}{V_{bed}} \tag{1.8}$$

$$\varepsilon_{gs} = \frac{W_I - W_S}{V_{bed}} \tag{1.9}$$

Porosity

The porosity of each packed bed material was determined volumetrically by initially draining the free water from the column for a period of 2 hours using a Cole-Palmer MasterFlex Model 7553-70 peristaltic pump (Vernon Hills, IL). Water was then slowly pumped upwards to an initial column level and recorded after settling for approximately 10 minutes. A controlled liquid volume within the packed bed column was drained and recorded, and the final water level was recorded approximately 20 minutes later. Tests were performed in triplicate for the 2.7 mm media, 3.5 mm media, and gravel layers.

RESULTS AND DISCUSSION

Mass-transfer coefficients

Average chemical constituents for both clean and dirty water are summarized in Table 1.3. Previous research has indicated the experimental K_La values increase with both the superficial water and air velocities (U_L and U_G) within a packed bed (Fujie et al. 1992; Ohshima et al. 1976, Alexander and Shah 1976). Overall, experimental results from the expanded clay and gravel layers tested, indicated that gas velocity has a stronger influence on the mass transfer coefficient than liquid velocity. Increases in the liquid temperature also resulted in a corresponding increase in the mass transfer coefficient, based on changes in liquid viscosity and diffusion kinetics. The mass transfer results are valid for temperatures in the range of 10 to 24 ^oC, U_G between 4 and 40 Nm/h, and U_L between 4 and 16 m/h. Figure 1.2 shows the clean water K_La values determined for the 2.7 mm media at the three liquid temperatures studied. K_La values measured at 10^{o}C, 16^{o}C, and 24^{o}C ranging from 40 to 200 h^{-1}, 50 to 270 h^{-1}, and 70 to 380 h^{-1}, respectively for clean water. The K_La values resulting from the dirty water testing measured at 10^{o}C and 24^{o}C ranged from 45 to 225 h^{-1} and 95 to 275 h^{-1}, respectively. A power regression of the K_La values determined at each water velocity resulted in discrete trends with all R^2 values greater than 0.9 in clean water and between 0.8 to 0.9 in dirty water. The K_La values for the 3.5 mm media at 10^{o}C ranged from 35 to 170 h^{-1} in clean water and 40 to 180 h^{-1} in dirty water. Correlations could again be made between the mass-transfer coefficient and superficial gas velocity with R^2 values greater than 0.9 for all superficial water velocities except at 16 m/h during the clean water

tests. The Type II gravel K_La values ranged from 13 to 165 h^{-1} in clean water and 42 to 155 h^{-1} in dirty water. The Type II gravel K_La values ranged from 16 to 98 h^{-1} in clean water and 22 to 93 h^{-1} in dirty water. Lower R^2 values were observed for the gravel and attributed to experimental error. As shown in Table 1.4, the range of K_La values found for the 2.7 mm and 3.5 mm media is within the ranges of those found in previous research for fixed bed systems using different types and sizes of media.

Table 1.3: Average dirty water chemical composition values

Parameter	**Clean Water**	**Dirty Water 10°C Testing**	**Dirty Water 24°C Testing**
pH	7.67	7.8±0.4	not tested
Alkalinity (mg/L as $CaCO_3$)	60	122±46	not tested
COD (mg/L)	not analyzed	40±10	51
DOC (mg/L)	2.1	8.3±2.0	8.4
NH_4-N (mg/L)	non-detect	non-detect	3.7
NO_2-N (mg/L)	non-detect	non-detect	non-detect
NO_3-N (mg/L)	2.5	6.6±0.9	4.8

Table 1.4: Comparison of mass-transfer coefficients with literature values

ε (-)	U_G (m/h)	U_L (m/h)	K_La (h^{-1})	Reference
0.29	4 – 40	4 – 16	40 – 380[3]	*This work*
0.35	4 – 40	4 – 16	35 – 170[3]	*This work*
0.43	6 – 36	6 – 36	5 – 135[1]	Reiber and Stensel (1985)
0.35 – 0.72	5 – 110	3 – 21	7 – 650[3]	Alexander and Shah (1976)
0.44 – 0.60	10 – 50	0.14-0.57	10 – 120[3]	Fujie et al. (1992)
[2]	18 – 216	36 – 216	25 – 240[3]	Ohshima et al (1976)

[1] Based on interstitial liquid volume in media
[2] Not available
[3] Based on void volume of media

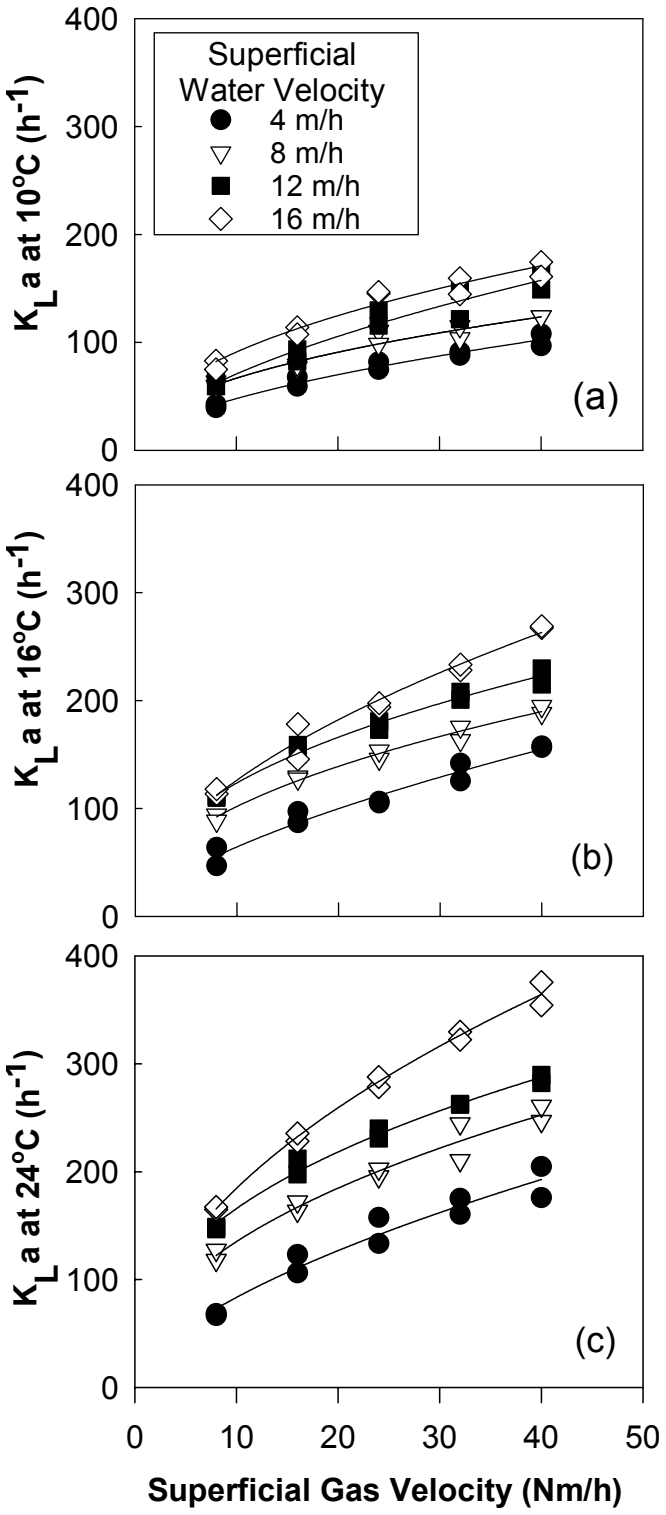

Figure 1.2: $K_La_{(T)}$ increases with increasing temperature in clean water for 2.7 mm media at (a) 10°C, (b) 16°C, and (c) 24°C.

Four and three replicates of a single testing condition established the reproducibility of the clean water oxygen transfer experiments at each temperature for the 2.7 mm and 3.5 mm media, respectively. The replicates were spaced throughout the testing period during each series of experiments. Based on the resulting K_La values, the overall coefficient of variation (standard deviation/mean) of the testing procedure was determined to be approximately a maximum of ± 12%. Therefore, greater than or equal to a ±12 % deviation is hereafter labeled as significantly different.

Media characteristics such as shape and grain diameter have also previously been shown to significantly affect oxygen transfer in a BAF (Moore et al. 2001, Kent et al. 2000). Accordingly, a comparison between the mass transfer coefficients and the two types of expanded clay tested was made. Significant differences were observed in the oxygen transfer dirty water testing at 10^oC for all but 4 of the full range of gas and liquid velocities. Significant differences were observed in the clean water testing at 10^oC for almost all of the testing conditions at the 2 lower liquid velocities but at only 2 testing conditions at the 2 higher liquid velocities. Overall, the results indicate that the two types of expanded clay media have different oxygen transfer characteristics based on the significance level set.

The temperature-dependent (θ) values obtained for the 2.7 mm media, Type I and Type II gravel were 1.046 $\pm$ 0.006, 1.025 $\pm$ 0.012, and 1.024 $\pm$ 0.013, respectively, based on Equation 1.4. Although the two gravel types agree with the commonly expected value of 1.024, the value for the 2.7 mm media is significantly higher. The K_La values from the 3 testing temperatures could then be adjusted to a standard temperature of 20^oC.

The dirty-water correction factor (alpha) for the 2.7 mm media was determined to be 1.3 $\pm$ 0.2 and 0.7 $\pm$ 0.1 for the 10^oC and 24^oC liquid temperatures, respectively. The dirty-water correction factor for the 3.5 mm media was determined to be 1.0 $\pm$ 0.2 at 10^oC. Dirty-water correction factors obtained for Types I and II gravel were determined to be approximately 1.1 $\pm$ 0.3 and 1.3 $\pm$ 0.3, respectively at 16^oC. The alpha values are close to 1.0, as found by Reiber and Stensel (1985) for both a synthetic wastewater and the wastewater effluent from their biologically active column. Fujie et al. attributed alpha values less than 1.0 to the

coalescence of bubbles as the microbial concentration increased (1992). In summary, the K_La value has been found to successfully fit the following general equation for the series of tests performed:

$$K_La_{(T)}(\text{wastewater}) = (\alpha)\cdot(c)\cdot U_G^a \cdot U_L^b \cdot \theta^{(T-20)} \qquad (1.10)$$

Figure 1.3 shows the overall goodness of fit for the 2.7 mm media as predicted by Equation 1.10 when compared to the experimental mass transfer coefficients measured at each temperature. The correlation equation falls within 20 % of the observed values for the majority of the data. Figure 1.4 shows the predictive Equation 1.10 also falls within 15% of the observed values for the majority of the data collected for the 3.5 mm media. A theta value of 1.046 was assumed for the 3.5 mm media.

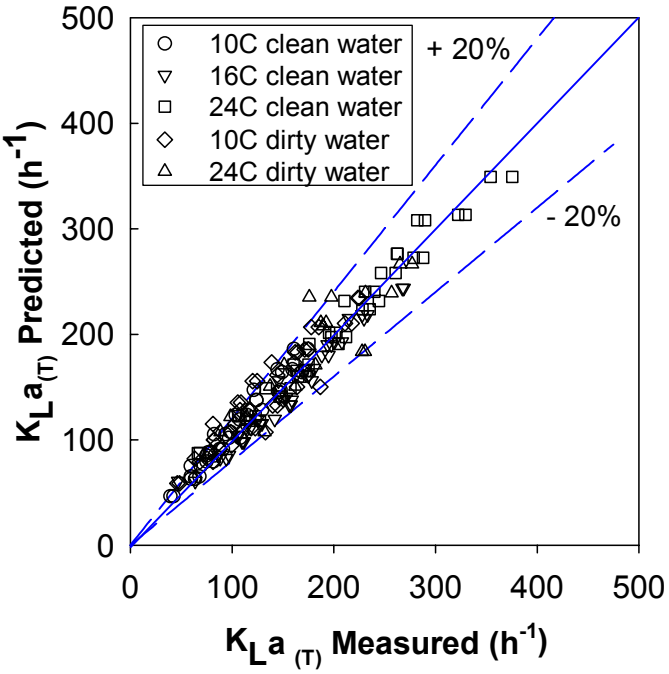

Figure 1.3: Overall goodness of fit for 2.7 mm media for K_La predicted with Equation 1.10 and K_La determined by fitting to Equation 1.3 with measured DO values.

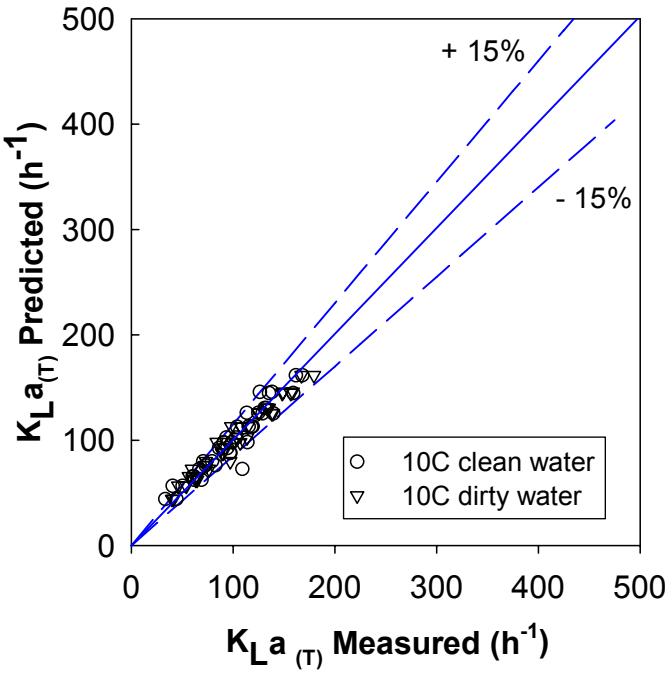

Figure 1.4: Overall goodness of fit for 3.5 mm media for $K_L a$ predicted with Equation 1.10 and $K_L a$ determined by fitting to Equation 1.3 with measured DO values.

Effect of gas holdup

Figure 1.5 shows a comparison of the total and stagnant gas holdup for the 2.7 mm media as a function of superficial gas velocity between the volumetric and gravimetric methods of measurement. The stagnant holdup is between 4.3 and 4.6% of the empty bed volume when measured volumetrically and between 4.5 to 5.2% of the empty bed volume when measured gravimetrically. The total gas holdup measured volumetrically is between 5.2% of the empty bed volume at the lowest gas velocity and 7.7% at the highest gas velocity and between 5.1% of the empty bed volume at the lowest gas velocity to 6.5% at the highest gas velocity when measured gravimetrically. Error bars representing one standard deviation are shown. Both methods produce comparable results, with differences falling within the range of experimental error. As observed by Ohshima et al. (1976) the stagnant gas holdup is independent of the gas flow rate for the range of values tested.

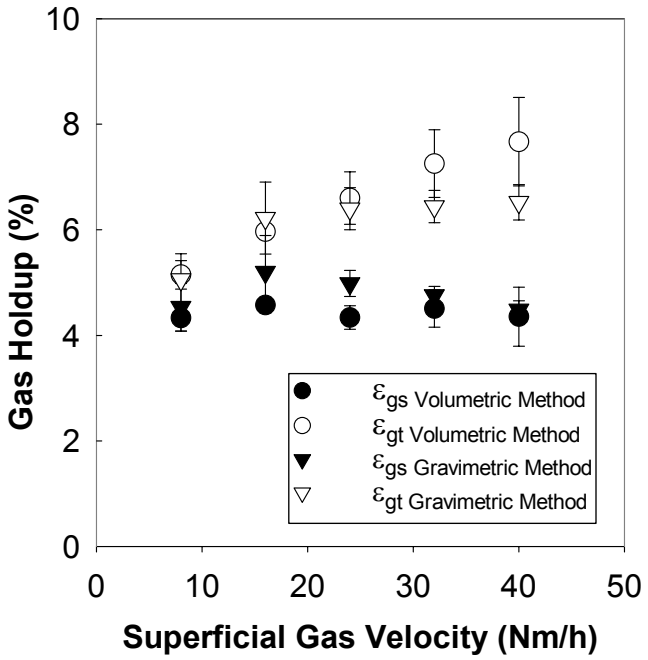

Figure 1.5: Independence of gas holdup fractions to liquid velocity but dependence of dynamic gas holdup to the gas velocity based on the comparison of methods in 2.7 mm media at 16°C. Data points from the gravimetric method were calculated by averaging the gas holdup at a given gas flow rate for the range of water.

Ohshima et al. (1976) observed a slight decrease in gas holdup with an increase in liquid velocities at similar rates. Increasing the liquid velocity in an upflow packed bed column produces an increase in the bed pressure. The process change would most likely produce a decrease in the retained gas volume. Although a slight decreasing trend in the total gas holdup may be present, the limited precision ($\pm$ 0.5%) prevents firm conclusions from being drawn. In addition, the similarity in the gas holdup fractions between the 2 methods of measurement further provides evidence of the negligible influence of the liquid velocity. For the experimental conditions evaluated, the seemingly negligible influence of the liquid velocity on gas holdup may be due to the relatively insignificant difference in pressure caused by the liquid velocity (the pressure being almost exclusively dictated by the height of media within the column rather than by the liquid velocity). However, in a full-scale column, the hydrostatic pressure at the bottom of the column would be higher than those experienced in the bench-scale column and may therefore have some impact on gas holdup. For example, the total gas holdup at the bottom of a full-scale BAF unit (assuming a 3.7 m media height)

could be about 1.5 times greater than the gas holdup at the top due to the difference in hydrostatic pressure.

Slight gas holdup fraction deviances were found in a comparison of the influence of liquid temperature on the 2.7 mm media. At a 10^{o}C water temperature, the stagnant gas holdup was 3.8% while the total gas holdup ranged from 3.9% to 5.9% using the gravimetric method. Using the volumetric method, the stagnant gas holdup was 4.6% while the total gas holdup fraction ranged from 5.2% to 7.4% at a 24^{o}C water temperature. The variations in gas holdup were found to fall within the range of experimental error and therefore deemed negligible.

A comparison of the influence of chemical constituents in the water on the total and stagnant gas holdup fractions within the 2.7 mm media showed a doubling of the stagnant gas holdup (see Figure 1.6). The 3.5 mm media showed the stagnant gas holdup fraction increased by a factor of 1.6. Based on gravimetric testing, the stagnant gas holdup was determined to be approximately 3.5% of the empty bed volume in clean water, but approximately 5.6% in the dirty water testing. The presence of surfactants in the dirty water may explain the increase in the stagnant gas holdup for both types of expanded clay media. Also, the 2.7 mm media may provide a more torturous path for the gas bubbles within the column.

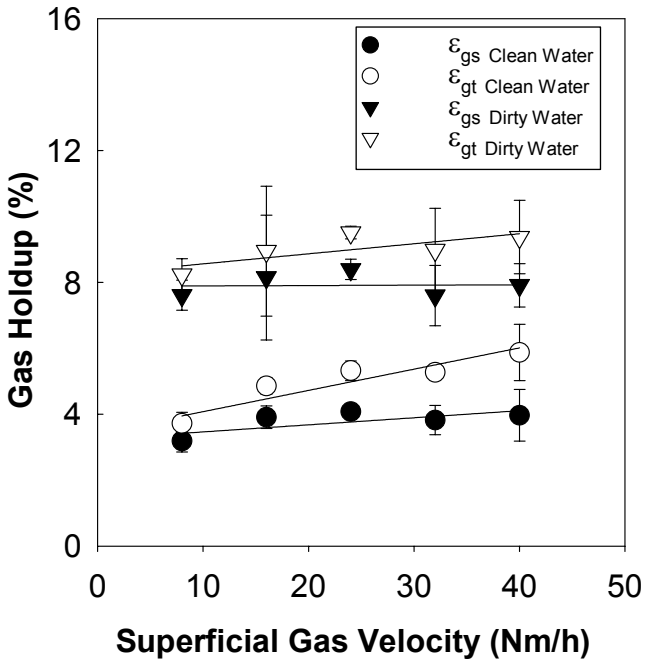

Figure 1.6: Effect of stagnant (doubled) and dynamic (negligible) gas holdup fractions between clean and dirty water at 10°C for 2.7 mm media.

Oxygen transfer as a function of gas holdup

The total gas holdup determined in clean and dirty water tests were found to have similar increasing slopes as a function of the superficial gas velocity for both the 2.7 mm and 3.5 mm media – indicating the fraction between the total and the stagnant gas holdup (dynamic) was independent of the chemical constituents in the water. The dynamic gas holdup increased from 0.7% at the lowest gas flow rate to 2.4% at the highest gas flow rate for both the 2.7 mm and 3.5 mm media. Similar trends were observed using both methods of measuring gas holdup. Other researchers have shown that the dynamic gas holdup serves as the primary determinant of the available interfacial area for mass transfer between the gas and the liquid (Fujie et al. 1992, Ohshima et al. 1976). The relative effect of stagnant gas bubbles on oxygen transfer was determined in clean water in additional transient testing of the 2.7 mm media. A rough estimate of the effect of the stagnant gas holdup on the K_La mass transfer value can be examined by plotting the slope of the oxygen reaeration curve in the flowing water immediately after closing the nitrogen gas feed (see Figure 1.7). The approximation can be obtained from the equation:

$$K_L a = \frac{J_{O2}}{C_{avg}} \tag{1.11}$$

The calculations revealed that the stagnant $K_L a$ is between 9 h^{-1} and 16 h^{-1} for all three testing temperatures for the range of liquid flowrates (17 total independent testing runs), or approximately a maximum of 15 to 20% of the value obtained in the oxygen transfer tests including both stagnant and dynamic gas holdups. Hence, it can be concluded that an increase in the superficial gas velocity would cause a proportional increase to the mass transfer values primarily as a function of the dynamic gas holdup fraction.

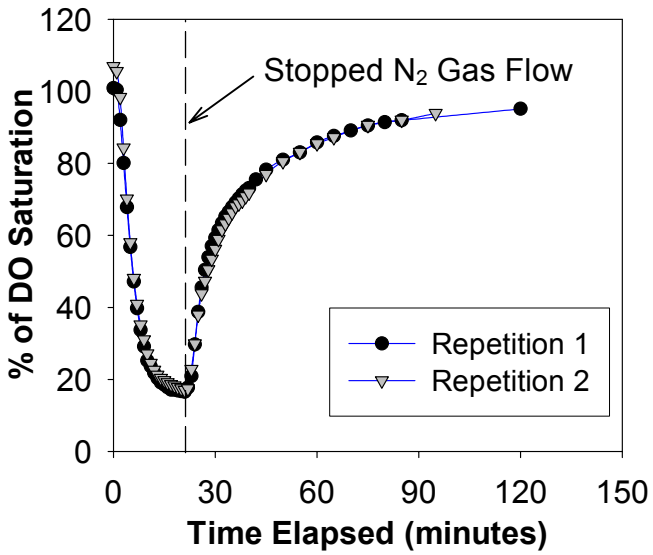

Figure 1.7: Minor effect of the stagnant gas holdup fraction on the oxygen mass transfer rate at 16°C.

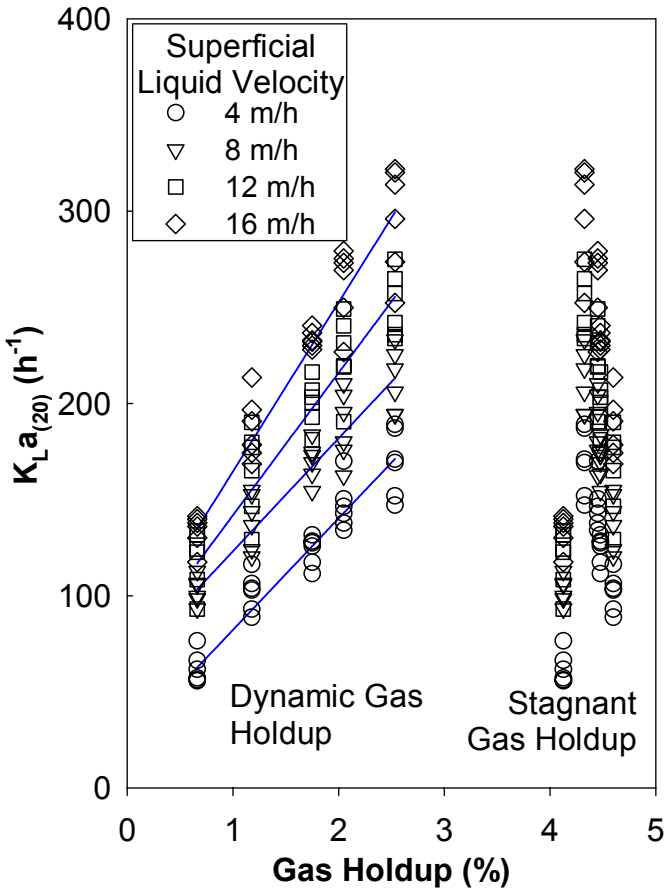

Figure 1.8: Direct proportionality of dynamic gas holdup on the mass-transfer coefficient in clean water for 2.7 mm media.

Figure 1.8 shows that the previously determined experimental K_La values for the 2.7 mm media is directly proportional to the dynamic gas holdup. Further insight is provided in Figure 1.9 which relates the K_La values expressed in terms of liquid volume to the interstitial liquid velocity. In contrast to using void volume as the basis for the mass-transfer coefficient, the liquid volume basis takes into account the displacement of liquid when the total gas holdup increases. K_La is a lumped parameter comprising K_L, the mass transfer coefficient, and a, the specific interfacial area. A partial understanding of these individual quantities can be gained by considering Figure 1.9. When based on the more fundamental liquid volume, K_La increases almost in direct proportion to dynamic gas holdup for a given U_L. This suggests that the dynamic holdup has a strong influence on the available interfacial area for mass transfer. One problem with the inference is that gas holdup is a volumetric quantity and the associated interfacial area would not be expected to increase linearly with an

increase in gas volume. As shown in Figure 1.9, K_La is also directly proportional to the interstitial liquid velocity, U_{IL}, provided that U_G is constant. This suggests that the interstitial liquid velocity controls the mass transfer coefficient, K_L, because the dynamic gas holdup is essentially independent of water flow rate. Ohshima et al. (1976) concluded that K_L only had a very slight dependence on U_L but increased more dramatically with dynamic gas holdup for larger packing media.

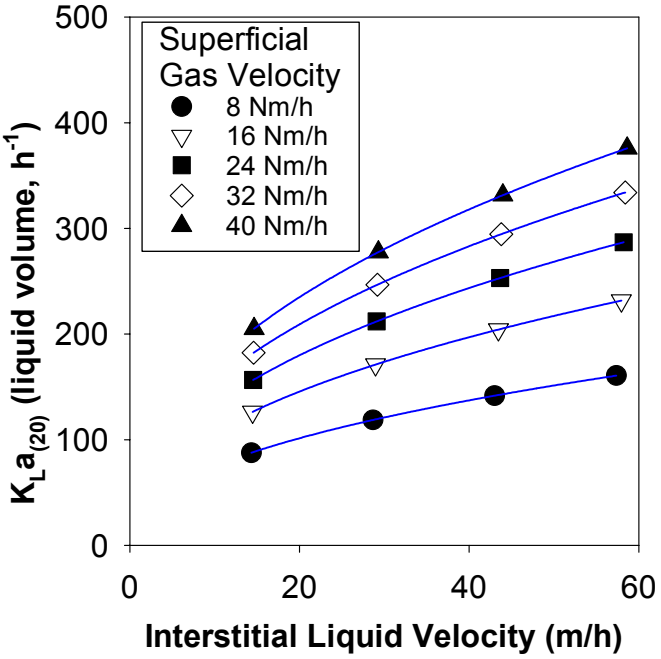

Figure 1.9: Direct increase of $K_La_{(20)}$ when based on the available specific interfacial area between the bubble and the liquid for 2.7 mm media.

CONCLUSIONS

The following conclusions can be drawn for the range of conditions investigated:

1. Mass-transfer coefficients were found to correlate well with the superficial gas velocity, the superficial liquid velocity, liquid temperature, and alpha factor.
2. Both the volumetric and the gravimetric method of measuring gas holdup produce similar results, indicating that liquid velocity does not have a significant impact on gas holdup.
3. Liquid temperature does not have a significant impact on gas holdup.
4. Stagnant gas holdup does not significantly influence the rate of oxygen transfer.

5. Although the dynamic gas holdup is independent of the chemical composition of the water, the stagnant gas holdup in the dirty water was roughly double that measured in clean water.
6. The mass-transfer coefficient is directly proportional to the dynamic gas holdup apparently because it influences the available interfacial area for oxygen transfer.

ACKNOWLEDGEMENTS

Funding was provided by Degremont North American Research and Development Center, Inc. (DENARD) and Virginia's Center for Innovative Technology. We acknowledge the assistance of Julie Petruska and Jody Smiley of Virginia Tech as well as Brandon Flint and Gregory Brazeau in the successful completion of the experimental work. We would also like to acknowledge the Blacksburg and VPI Sanitation Authority Lower Stroubles Creek Wastewater Treatment Facility in Blacksburg, VA as well as the Roanoke Water Pollution Control Plant in Roanoke, Virginia for their assistance in supplying secondary effluent for the study.

REFERENCES

ASCE. *Standard Guidelines for In-Process Oxygen Transfer Testing*. New York, NY: American Society of Civil Engineers Oxygen Transfer Standards Subcommittee. 1997.

APHA-AWWA-WPCF. *Standard methods for the examination of water and wastewater*, 20th Ed., Washington DC. 1998.

Alexander, B. F. Shah Y. T. Gas-liquid mass transfer coefficients for cocurrent upflow in packed beds. *J. Can. Chem. Eng.* 1976; 54:556-559.

Brown, L. C. Baillod C. R. Modeling and interpreting oxygen transfer data. *Environmental Engineering Division, Proceedings of the American Society of Civil Engineers*: ASCE. August 1982; 108.

Capela, S. Gillot S. Heduit A. Oxygen transfer under process conditions: comparison of measurement methods. *Proceedings of the WEF 72nd Annual Conference and Exposition*; New Orleans, LA. 1999.

Danill, E. I. Gulliver J. S. Temperature dependence of liquid film coefficient for gas transfer. *J. Env. Eng*. 1988; 114(5):1224-1229.

Fujie, K. Hu H. Y. Ikeda Y. Kohei U. Gas-liquid oxygen transfer characteristics in an aerobic submerged biofilter for the wastewater treatment. *Chem. Eng. Sci*. 1992; 47(13-14):3745-3752.

Goto, S. Saikawa K. Gaspillo P. Mass transfer and holdup in gas-liquid cocurrent flow packed beds containing water-repellent particles. *Canadian Journal of Chemical Engineering*. 1991 Dec; 69:1344-1347.

Groves, K. P., Daigger, G. T., Simpkin, T. J., Redmon, D. T., Ewing, L. "Evaluation of oxygen transfer efficiency and alpha-factor on a variety of diffused aeration systems." *Water Environment Research*, 64(5), 1992; 691-698.

Harris, S. L. Stephenson T. Pearce P. Aeration investigation of biological aerated filters using off-gas analysis. *Wat. Sci. Tech*. 1996; 34(3-4):307-314.

Iranpour, R. Magallanes A. Zermeno M. Varsh V. Assessment of aeration basin performance efficiency: Sampling methods and tank coverage. *Wat. Res*. 2000; 34(12):3137-3152.

Kent, T. D. Williams S. C. Fitzpatrick C. S. B. Ammoniacal nitrogen removal in biological aerated filters: The effect of media size. *J.CIWEM*. 2000 Dec; 14:409-414.

Linek, V. Vacek V. Chemical engineering use of catalyzed sulfite oxidation kinetics for the determination of mass transfer characteristics of gas-liquid contactors. *Chemical Engineering Science*. 1981; 36(11):1747-1768.

Leung, S.M. Little, J.C. Love, N.G. Measurement of oxygen uptake in a nitrifying biological aerated filter. 2003. *to be submitted for publication*.

Little, John C. Hypolimnetic aerators: predicting oxygen transfer and hydrodynamics. *Water Res*. 1995; 29:2475-2482.

Mendoza-Espinosa, L. and Stephenson T. A review of biological aerated filters (BAFs) for wastewater treatment. *Env. Eng. Sci*. 1999; 16(3):201-216.

Moore, R. Quarmby J. Stephenson T. The effects of media size on the performance of biological aerated filters. *Wat. Res*. 2001; 35(10):2514-2522.

Ohshima, S. Takematsu T. Kuriki Y. Shimada K. Suzuki M. Kato J. Liquid-phase mass transfer coefficient and gas holdup in a packed-bed cocurrent up-flow column. *J. Chem. Eng., Japan.* 1976; 9(1):29-34.

Peladan, J. G. Lemmel H. Pujol R. High nitrification rate with upflow biofiltration. *Wat. Sci. Tech.* 1996; 34:347-353.

Pelkonen, M. Upgrading oxygen transfer in the activated sludge process. *Wat. Sci. Tech.* 1990; 22(7-8):253-260.

Pujol., R. Hamon M. Kandel X. Lemmel H. Biofilters: Flexible, reliable biological reactors. *Wat. Sci,. Tech*. 1994; 29:33-38.

Reiber, S. Stensel D. Biologically enhanced oxygen transfer in a fixed-film system. *J. Water Pollut. Control Fed.* 1985; 57(2):135-142.

Rogalla, F. Payraudeau M. Bacquet G. Bourbigot M. Sibony J. Gilles P. Nitrification and phosphorus precipitation with biological aerated filters. *J. Water Pollut. Control Fed*. 1990; 62:169-176.

Ruchti, G. Dunn I. J. Bourne J. R. Practical guidelines for the determination of oxygen transfer coefficients (K_La) with the sulfite oxidation method. *Chemical Engineering Journal*. 1985; 30:29-38.

Stensel, H. D. Brenner R. C. Lee K. M. Melcer H. Rakness K. Biological Filter Evaluation. *J. Env. Eng.* 1988; 114:655-671.

Tchobanoglous, G., Burton, F. L., and Stensel, H. D. *Wastewater Engineering: Treatment and Reuse.* Metcalf & Eddy. New York. 2003. p. 438.

MANUSCRIPT 2: MEASUREMENT OF OXYGEN UPTAKE IN A NITRIFYING BIOLOGICAL AERATED FILTER

SUSANNA M. LEUNG, JOHN C. LITTLE and NANCY G. LOVE

Department of Civil and Environmental Engineering, Virginia Polytechnic Institute and State University, Blacksburg, Virginia 24061-0246, USA

ABSTRACT –A tertiary nitrification biological aerated filter (BAF) pilot unit was operated for 5 months downstream of a secondary treatment unit at a domestic wastewater treatment facility. The purpose of the study was to investigate the oxygen transfer capabilities of the nitrifying unit with high oxygen demand requirements through a series of aeration process tests and to explore the presence of oxygen transfer enhancements by further analyzing the actual transfer mechanism limitations. It was determined that assuming an OTE factor of 20%, aerating the BAF pilot unit based on the stoichiometric aeration demand resulted in overaeration of the unit, especially at lower pollutant loading rates. Endogenous respiration contributed to only 2 – 7% of the total oxygen demand with the regions of biomass activity changing with varying loading conditions. An enhanced oxygen transfer factor was determined in the biologically active pilot. Although it cannot be definitively concluded that the observed oxygen transfer factor is either due to biological activity or not simply an artifact of measurement/analysis techniques, the enhancement factor can be accounted for by either an increase in the K_La factor or the associated driving force using a proposed enhanced bubble theory.

Key words – BAF, nitrification, aeration, DO gradient, biological oxygen transfer enhancement, bubble enhancement

NOMENCLATURE

a	empirical factor of U_G for the predicted K_La determination
A	surface area of bed (m^2)
b	empirical factor of U_L for the predicted K_La determination
b_{CD}	assumed elongated cylindrical bubble diameter (m)

b_{CL} assumed elongated cylindrical bubble length (m) = $(2b_{SD}^3/3b_{CD}^2)$

b_{SD} assumed spherical bubble diameter (cm)

c empirical factor for the predicted K_La determination

C bulk oxygen concentration (mg/L)

C_{bulk} DO concentration measured in the bulk process water (mg/L)

C_{BL} calculated average DO concentration in boundary layer (mg/L)

$C_{consumed}$ DO concentration biologically consumed (mg/L)

C_{sat} saturated oxygen concentration at the gas-liquid interface (mg/L)

COD chemical oxygen demand (mg/L)

DOC dissolved (< 0.45 μm) organic carbon (mg/L)

H depth of water in the column (meters)

J oxygen flux (mg/L/h)

K_La_T liquid mass transfer coefficient based on void volume at given temperature (h^{-1})

L_T squeezed water film thickness between biofilm and air bubble (m)

m Henry's law constant

M molar mass of oxygen (32 g/mol)

m_{SA} specific surface area of 2.7 mm media (1950 $m^2$of surface area/m^3 of media)

NH_4-N readily bioavailable ammonium concentration as nitrogen (mg/L)

NO_2-N nitrite concentration as nitrogen (mg/L)

NO_3-N nitrate concentration as nitrogen (mg/L)

O assumed value for the variable of interest

O_{BL} baseline determination value of the variable of interest

OTE oxygen transfer efficiency

P 100,000 Pa/bar

P_t total hydrostatic pressure (bar)

PA assumed parameter value

PA_{BL} baseline determination value of the parameter

Q process liquid flow rate (m^3/h)

Q_{bw} backwash liquid flow rate (m^3/h)

r_{bio} assumed biofilm oxygen consumption rate (g/m^3s)

S_e soluble NH_4-N concentration in composite effluent (mg/L)

S_o total NH_4-N concentration in composite influent (mg/L)

S_R relative sensitivity

t_{bw} backwash waste sampling duration (minutes)

T temperature (^{o} Celsius)

TSS total suspended solids (mg/L)

U_G superficial gas velocity based on empty bed at 1 atm and 20^{o}C (Nm/h)

U_L superficial liquid velocity based on empty bed (m/h)

V_b bubble rise velocity (cm/s)

VSS volatile suspended solids (mg/L)

$X_{sloughed}$ ammonium-nitrogen bound to biomass slough in composite effluent (mg/L)

X_i inert organic particulates in composite influent (mg/L)

Xn ammonium-nitrogen bound to particulate matter in the composite influent (mg/L)

X_T total COD concentration in backwash waste sample (mg/L as COD)

y_{out} mole fraction of oxygen in the gas-phase at a given height of the pilot

Y_{obs} observed 48 hour biomass yield (mg COD/mg NH_4-N removed)

z distance of water travel up the column from gravel/media interface (m)

α $\frac{K_L a_{wastewater}}{K_L a_{clean\ water}}$ correction factor ratio

β $\frac{DO_{sat\ wastewater}}{DO_{sat\ clean\ water}}$ correction factor ratio

ε bed porosity

ρ O_2 density in dry air at standard conditions (300 mg O_2/L of air)

θ dimensionless constant for temperature correction

θ_μ overall kinetic dimensionless constant for temperature correction

θ_{cycle} duration of filtration time in pilot unit (minutes)

INTRODUCTION

Biological aerated filtration (BAF) processes provide a favorable environment for the development of a densely populated active biomass attached to and entrapped in a porous support media. Wastewater typically flows upwards through BAF units and oxygen is provided by bubbling air through the biomass-laden porous media for aerobic systems.

BAFs are particularly well suited for nitrification due to the inherent low biological growth rates and high oxygen requirements demanded by nitrifiers. In a full-scale comparison between conventional activated sludge and a BAF unit in Denmark, Thogersen and Hansen (2000) concluded that BAFs provided more complete ammonium removal than the activated sludge process, especially at low water temperatures. Also, in a comparison with suspended growth systems, BAFs require minimal time for recovery from process shutdown and microbial activation due to changing process conditions (Poughon et al., 1999; Ydstebo et al., 2001).

Despite the advantages, the BAF process remains somewhat of a black box in wastewater treatment. The biomass and its mechanistic influence in a fixed-film process environment are not fully comprehended. Although published micro and macro-scale models incorporate key interaction parameters explaining the overall microbial behavior, researchers have made simplifying assumptions on even some of the most fundamental aspects of the system (Jacob et al., 1997; LeTallec et al., 1999; Mann and Stephenson, 1997; Poughon et al., 1999; Rittmann and Manem, 1992; San et al., 1993; Saez and Rittmann, 1988). In particular, the high aeration demands in the aerobic biological process warrant a closer look for optimization (Mendoza-Espinosa and Stephenson, 1999).

The major factors that influence the oxygen transfer efficiency (OTE) within BAF systems include gas velocity, bulk dissolved oxygen (DO) concentration, surfactants, ionic strength, and diffusion kinetics. Traditional biofilm oxygen transfer models for bacterial uptake include diffusion as a multi-step process. Oxygen transfer rates at the gas/liquid interface are driven by the difference between the oxygen available in the gas phase and the DO concentration in the liquid phase. Increasing the difference between the two concentrations can significantly increase the pollutant removal capacity of a nitrifying BAF unit (Ydstebo et al., 2001).

A recent review concluded that, in particular, the biofilm in a BAF has a significant positive effect on oxygen transfer efficiency which suggests the possibility for biological oxygen transfer enhancement (BOTE) (Mendoza-Espinosa and Stephenson, 1999). The presence of

BOTE has been suggested in activated sludge, rotating biological contactors, and fermentation processes with many researchers agreeing to the presence of a separate oxygen transfer mechanism in biological systems that cannot be accounted for in traditional diffusion kinetics (Ju and Sundararajan, 1992; Mines and Sherrad, 1985; Lee and Stensel, 1986; Harris et al., 1996; Sundararajan and Ju, 1995; Reiber and Stensel, 1985). Albertson and DiGregorio (1975) proposed the enhancement is a result of direct oxygen transfer between the gas phase and bacterial flocs. Tsao (1968) proposed that traditional oxygen transfer kinetics cannot be spatially separated in aerobic fermentation processes and instead, there is an overlap between the gas-liquid interfacial film and the active bacterial cell film. In addition, the theory postulates that instead of a stagnant layer, surfactant and biomass material which concentrate at the interfacial layer are continuously exchanged between the interface and bulk liquid. Lee and Stensel (1986) modified the theory by Tsao for fixed-film growth, with the steep oxygen gradients at and near the interface of a biofilm.

In other BAF systems, an overall rate of oxygen transfer 1.2 to 3.2 times above the rate that would be expected for diffused aeration alone was determined with the presence of a biologically active biofilm. The studies of the BAF systems also found increasing enhancement factors corresponding to increases with the biomass concentration, pollutant removal load and available interfacial surface area (Harris et al., 1996; Lee and Stensel, 1986; Reiber and Stensel, 1985). The presence of the media bed has been shown to minimize bubble coalescence as well as to increase the gas retention time within the bed (Fuije et al., 1992). Yet, some researchers also question the existence of oxygen transfer enhancement. The enhancement phenomenon observed in biological systems does not coincide with the traditional retardation in oxygen transfer factors when comparing wastewater to clean water (Iranpour et al., 2000; Pelkonen, 1990). In addition, oxygen transfer determinations can vary significantly based on process conditions and between in-situ sampling and ex-situ analysis of samples (Mueller and Stensel, 1990). Still others determined that the traditional kinetics can account for oxygen transfer even in the presence of biomass (Nogueira et al., 1998; Vaxelaire et al., 1995)

Although a number of researchers have attempted to study the substantial potential enhancement in the oxygen transfer rate in biological processes, the actual transfer mechanism limitations are still not well understood. Reliable methods of measuring oxygen transfer and the variability of scaling up data from bench-scale units are still points of contention. The specific objectives of the study were 1) to investigate the oxygen transfer capabilities of the nitrifying unit with high oxygen demand requirements through a series of aeration process tests and 2) to explore the presence of oxygen transfer enhancements calculated within the unit by further analyzing the actual transfer mechanism limitations.

MASS TRANSFER THEORY

Theoretical oxygen requirement

An initial aeration requirement for the tertiary unit can be roughly determined by estimating the theoretical oxygen demand required, where:

$$R_{Aeration\ Demand} = \left(r_{Endogenous\ Respiration} + r_{Applied\ NH_4 \cdot N} - r_{NH_4 \cdot N\ for\ biomass\ growth}\right)\left(\frac{Q}{\rho\ OTE}\right)\theta_{\mu}^{(20-T)} \qquad (2.1)$$

where

$$r_{Applied\ NH_4 \cdot N} = NH_4 \cdot N_{removed}\left(\frac{4.57\ g\ O_2}{g\ NH_4 \cdot N}\right) \qquad (2.2)$$

$$r_{NH_4 \cdot N\ for\ biomass\ growth} = Y_{obs}\ \left(NH_4 \cdot N_{removed}\right)\left(\frac{0.087\ g\ N}{g\ cell\ as\ COD}\right)\left(\frac{4.57\ g\ O_2}{g\ NH_4 \cdot N}\right) \qquad (2.3)$$

For a tertiary nitrification system, readily biodegradable COD levels and heterotrophic growth were assumed to be negligible. The rates of endogenous respiration ($r_{endogenous\ respiration}$) and observed autotrophic yield (Y_{obs}) were experimentally determined during testing to be 6.5 mg/L O_2 and 0.17 g cell as COD/g NH_4-N, respectively. In addition, several assumptions were made regarding the system, including an overall temperature correction factor ($\theta\mu$) to be 1.11 (Grady et al., 1999) and an oxygen transfer efficiency (OTE) to be 20% in the BAF unit.

Oxygen rate balance

The experimental net rate of oxygen transfer in the nitrification system can be expressed for a given sectional height within a BAF unit. The liquid phase oxygen mass transfer coefficient (K_La) from gas to liquid phase can then be calculated from the rate balance. To do this, the biomass is assumed to exert oxygen demand along the length of the bed column as if it were acting as an ideal plug flow reactor. Therefore, the dissolved oxygen concentration varies with respect to both time and height along the bed column media bed. In addition, negligible concentrations of influent solids, readily biodegradable COD levels, and heterotrophic growth were assumed to be introduced to the tertiary unit in the screened secondary effluent entering the system (see the *Pilot Unit Operation* section in *Experimental Methods* for details). Assuming steady state conditions, the dissolved oxygen concentration at a given location in the bed remained constant with respect to time, as shown in Equation (2.4):

$$\mathrm{R}_{\mathrm{O_2\ Accumulation}} = \mathrm{R}_{\mathrm{O_2\ Transfer\ from\ gas\ phase}} - \mathrm{R}_{\mathrm{O_2\ Net\ NH_4\ Oxidation}} + \mathrm{R}_{\mathrm{Endogenous\ Respiration}} \tag{2.4}$$

$$\text{where } \mathrm{R}_{\mathrm{O_2\ Net\ NH_4\ Oxidation}} = R_{\mathrm{NH_4\text{-}N\ Loss}} - R_{\mathrm{NH_4\text{-}N\ for\ biomass\ growth}} \tag{2.5}$$

The relationship can be rewritten as:

$$Q\,C_{z+\Delta z} - Q\,C_z = \alpha\,\varepsilon\,K_L a\left(\beta C_{sat} - C\right)A\,\Delta z - (r_N - r_G + r_E)\,A\,\Delta z \tag{2.6}$$

Manipulation of the Equation (2.6) then provides the oxygen transfer factor:

$$K_L a = \frac{\frac{\Delta C}{\Delta z}U_L + \left(r_N - r_G + r_E\right)}{\alpha\,\varepsilon\left(\beta C_{sat} - C\right)} \tag{2.7}$$

with the following supporting equations:

$$U_L = {}^{Q}\!/_{A} \tag{2.8}$$

$$\mathrm{C_{sat}} = \frac{\mathrm{y_{out}\ P_t}}{\mathrm{m}} \tag{2.9}$$

The total bed pressure at any given height within the pilot unit (P_t) was calculated based on the Rose Equation for determining headloss through the filter bed and the Bernoulli Equation

(Franzini and Finnemore, 1997; Tchobanoglous et al., 2003). Rose Equation Shape factor coefficients (Φ) of 0.82 and 0.73 were assumed for the gravel and expanded clay media bed, respectively.

$$\frac{y_{out}}{1-y_{out}} = \frac{y_{in}}{1-y_{in}} - \frac{(C_{out} - C_{in} + C_{demand})Q}{M\,G_o} \tag{2.10}$$

$$C_{demand} = r_N - r_G + r_E \tag{2.11}$$

$$Y_{obs} = \frac{(X_T - X_i)\,Q_{bw}\,t_{bw}}{(S_o - S_e - X_{sloughed} - X_n)\,Q\,\theta_{cycle}} \tag{2.12}$$

Due to the characteristics of the influent and effluent of the pilot unit (see the *Pilot Unit Operation* section in *Experimental Methods* for details), the inert organic particulates in the influent (X_i), inert ammonium-nitrogen bound in the particulate phase of the influent (X_n), and ammonium-nitrogen bound in the biomass sloughed into of the effluent ($X_{sloughed}$) terms in Equation (2.12) were assumed to be negligible.

$$r_N = \frac{Q}{A\Delta z}\left[\left(NH_4 \cdot N_{removed}\right)\left(\frac{4.57\ mg\ O_2}{mg\ NH_4 \cdot N}\right) + \left(NO_2 \cdot N_{removed}\right)\left(\frac{1.14\ mg\ O_2}{mg\ NO_2 \cdot N}\right)\right] \tag{2.13}$$

$$r_G = \frac{Q}{A\Delta z}\left[\left(Y_{obs}\right)\left(NH_4 \cdot N_{removed}\right)\left(\frac{0.087\ mg\ N}{mg\ cell\ as\ COD}\right)\left(\frac{4.57\ mg\ O_2}{mg\ NH_4 \cdot N}\right)\right] \tag{2.14}$$

$$r_E = \frac{Q}{A\Delta z}\left(\Delta C\right) \tag{2.15}$$

$$m \propto 10^{-(J/T)} \tag{2.16}$$

Henry's law constant "m" is temperature dependent, where J is a temperature correction coefficient and T is absolute temperature. For oxygen, m = 0.0229 bar/(g/m^3) at 20^{o}C and J = 730 K (Selleck et al., 1988).

EXPERIMENTAL METHODS

Overview

A pilot-scale upflow BAF was installed at a 102 million-liter per day municipal wastewater facility. The BAF pilot unit consisted of flanged carbon steel pipe sections (0.91 m I.D.) that were connected to a total height of approximately 6 meters as shown in Figure 2.1. The influent wastewater entered a 0.91 m deep underdrain section contained by a carbon steel plate with liquid diffusers that provided uniform liquid flow up through the pilot unit. A coarse bubble diffuser system was located immediately above the steel plate and provided aeration to the unit. Both the liquid and air diffusers were covered by 0.35 m of 1.9 to 2.5 cm diameter support gravel underneath an additional 0.15 m of 0.9 to 1.9 cm diameter support gravel. Approximately 3.7 m of angular-shaped, thermally-expanded porous clay media with an effective size of 2.7 mm was added above the support gravel. At 1.2 m intervals spaced regularly along the height of the 2.7 mm media bed, 4 permanent liquid sampling sites were installed to enable chemical bed profile characterizations. Sampling Port 1 was located at the interface between the support gravel and the 2.7 mm media bed while sampling Port 4 was located inches below the top of the 2.7 mm media bed.

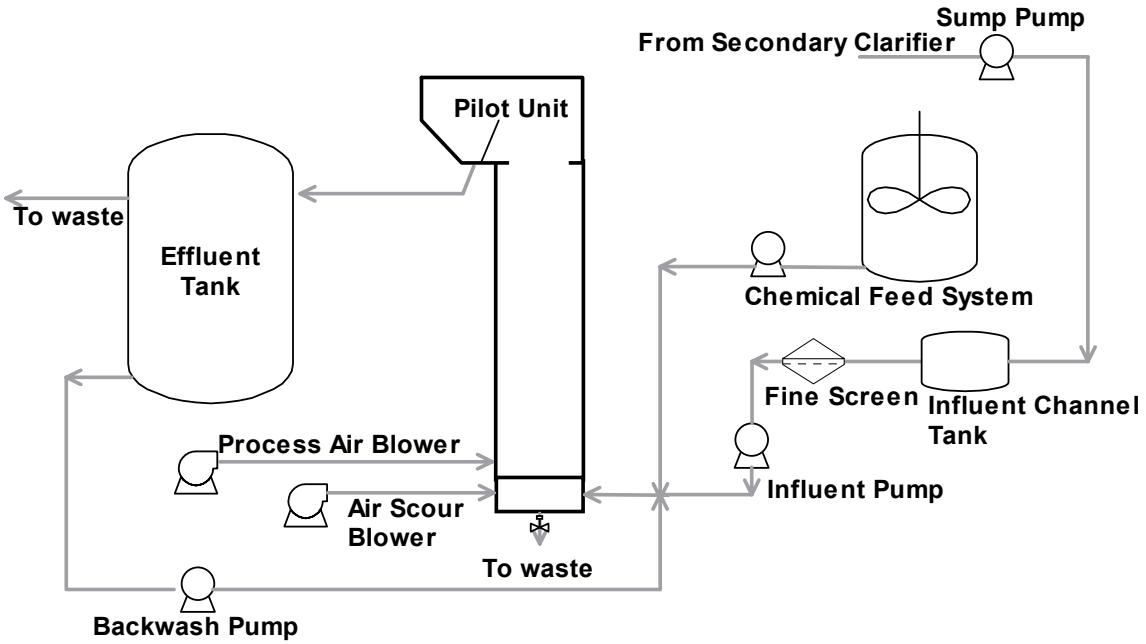

Figure 2.1: Overall pilot unit schematic. Valves and instrumentation are not shown.

Pilot unit operation

The BAF pilot unit was biologically seeded using activated sludge from an aeration basin at the wastewater treatment facility. During the startup time period, the BAF operated for a period of 8 weeks under conditions where sufficient oxygen was provided at a superficial water velocity of 4.0 m/h and an inlet ammonium-N concentration of approximately 45 mg/L. The pilot was regularly backwashed three times a week, following either 48 or 72 hour of continuous operation of the filter (filter run cycles), consisting of a series of air scours and upflow water rinses. Regularly scheduled backwashes allowed for the release of excess biomass accumulated during the previous filter run and prevented biomass and bound ammonium-N from sloughing in the effluent during filtration. The unit continuously received screened (2.5 mm) secondary effluent from the overflow of an adjacent secondary clarifier. Due to the consistently low concentrations of biologically available carbon (32 $\pm$ 4 mg/L of total COD) and total suspended solids (<10 mg/L) in the source water, heterotrophic growth was kept to a minimum in the pilot unit and the slower growing nitrifying community was allowed to predominate the media bed. In addition, the secondary effluent originally contained non-detectable levels of ammonium and approximately 106 $\pm$ 60 mg/L of alkalinity. The lack of suspended solids present in either the pilot influent or effluent provided the basis for assuming the inert organic particulates in the influent (X_i), inert ammonium-nitrogen bound in the particulate phase of the influent (X_n), and ammonium-nitrogen bound in the biomass sloughed into of the effluent ($X_{sloughed}$) terms in Equation (2.12) were negligible. All ammonium and additional concentrations of alkalinity were supplemented exogenously to the unit with food-grade ammonium bicarbonate and sodium bicarbonate to mimic a tertiary nitrification filter.

A supplemental chemical feed system was composed of a covered 1,325 L Nalgene tank, Lightnin (Rochester, NY) rapid mixer, LMI Milton Roy (Acton, MA) chemical metering pump, and 13 mm I.D. flexible vinyl tubing. A batch process was used to make up the chemical feed stock solution by adding equal weights of the two supplements to an approximate concentration of 100 g/L of ammonium as nitrogen. Both precipitation and formation of a concentration gradient within the feed tank were prevented by the rapid mixer, and the stock solution was remade every 5 days.

Aeration testing

Aeration testing occurred over a period of three months. The aeration testing matrix was designed to observe both nitrification and oxygen transfer characteristics under a broad range of conditions. The pollutant and hydraulic loadings were varied and corresponded with different aeration requirements, as shown in Table 2.1. All loading rates are hereafter defined in units of kilograms of given pollutant per cubic meter of 2.7 mm media per day. Targeted effluent loadings for each Test Condition were based on the half-saturation coefficient for ammonium-N of 1.0 mg/L (Grady et al., 1999). For each given Test Condition, an initial baseline evaluation of the biological state of the pilot unit was conducted at an aeration rate achieving the required nitrification loading. A theoretical aeration requirement for the given ammonium loading was determined using Equation (2.1) with an assumed OTE of 20%. The pilot unit was allowed to stabilize at each aeration rate for a period of approximately 20 hours before testing occurred. After full nitrification was experimentally verified, a step protocol was implemented to determine the lowest aeration rate required to maintain the desired ammonium removal percentages, if the target was not achieved, an oxygen-limited state in the unit was assumed. Using a refrigerated composite sampler system, eight (8) hour composite samples of the influent and effluent were each collected immediately prior to testing. The composite samples provided a basis for determining the lowered aeration rate for the following day and served as a comparison between the nitrification capacity of the system hours before and during testing. Samples were kept in a cooler for transport to the laboratory and analyzed as outlined in Table 2.2**.**

Table 2.1: Pilot ammonium and hydraulic loadings and performance criteria for aeration testing matrix.

Test Condition	Velocity [m/h]	Inlet NH_4-N [mg/L]	NH_4-N Loading Rate [kg N/m^3/d]	Targeted Maximum Effluent NH_4-N Load [kg N/m^3/d]	Theoretical Aeration Requirement [Nm/h]
1	4.0	45	1.1	0.03	8.6
2	15.0	15	1.4	0.10	15.2
3	7.6	30	1.5	0.05	18.0
4	10.4	15	1.1	0.07	13.9
5	5.0	45	1.5	0.03	25.1

In order to minimize variations in the physical and biological reactor environment, profile sampling commenced between 18 hours and 55 hours into a filter run. The unit was backwashed 1 day prior to the first aeration rate testing for a given Test Condition. Backwashing then commenced again immediately after profile sampling at the second and, if necessary, the fourth aeration rate for the same Test Condition. The method allowed for normal operation filter run times but avoided anomalies that might be due to residual effects from backwash. After finishing the series of aeration rate testing for a given Test Condition, the pilot was set at the next Test Condition as defined in Table 2.1. A minimum of a week was allowed for the unit to reach stable operation at full nitrification again. The next series of aeration testing began after composite influent and effluent samples verified the unit had acclimated to the new Test Condition.

Table 2.2: Summary of standard sample testing parameters. The testing method is implied from the Standard Methods (APHA, 1998) reference unless otherwise stated.

Standard Test Parameter	Method*	Routine Operation	Aeration Testing	Endogenous Respiration	Biological Yield-Backwash	Biological Yield-Filter
pH	4500-H^+-B	X	X	X		X
Alkalinity	2320B	X	X	X		X
NH_4-N	HACH AmVer® Test N' Tube	X	X	X		X
NH_4-N	4500-NH_3C		X			X
NO_2-N	4500-NO_2^-B	X	X	X		X
NO_3-N	CHEMetrics CHEMets® ampules	X				
NO_3-N	4500-NO_3^-C		X	X		X
sCOD	5220C				X	X
tCOD	5220C		X		X	X
DOC	5310C		X			
TSS	2540D				X	
VSS	2540E				X	

During each day of aeration testing, a bulk dissolved oxygen (DO) profile was recorded at each of the six heights along the column and individual 500 mL grab samples were collected for chemical analysis. Liquid samples were obtained from six separate locations along the pilot column: the influent side port used to obtain composite samples, the 4 sampling ports

located within the 2.7 mm media, and at the effluent weir. The four stainless steel 6.4 mm I.D. sampling pipes were installed horizontally across the entire diameter of the column at each of the sampling ports along the media bed. Each pipe could obtain radially representative liquid samples from the center 25 centimeters of the unit for chemical analysis and bulk water DO readings. The top-side of the sampling pipes contained a series of 10 small holes to obtain bubble-free liquid samples and to minimize opportunities for clogging. Bubbles were further discouraged from entering the sampling pipes due to the presence of steel "deflectors", welded strips angled outwards on either side of the length of the drilled sampling holes. Each sampling pipe was connected to a tee once outside the column to allow the release of any air bubbles, which had entered the sampling pipe. Standard 6.4 mm I.D. vinyl tubing connected the tee to a sampling manifold located at the base of the unit. In order to simplify sampling by a single operator, each sample line was connected to an individual 6.4 mm PVC manual ball valve to control flow from the manifold. All flexible tubing was wrapped with duct tape to minimize the growth of algae and other light dependent organisms.

During sampling, representative water samples from the 4 media and influent ports along the column were extracted from the sample tubes of the sampling manifold through 6.4 mm I.D. vinyl tubing to measure dissolved oxygen in a 60 mL magnetically-stirred, flow-through sample cell at controlled flow rates of 200 to 500 mL per minute. The length of the vinyl tubing to the sample cell introduced a negligible sample time delay. Dissolved oxygen measurements (Yellow Springs Instrument Co., Inc., OH, Model 55 meter) were recorded using a standard membrane after a minimum of 3 liquid residence times had flushed the cell, and the readings stabilized (approximately 5 to 10 minutes). The water in the cell was completely mixed and sealed from any air-water transfer by the gasketed dissolved oxygen probe fitting. Individual 500 mL samples taken from each sampling site during testing were stored in a cooler for transport until analysis.

Media porosity

Determination of the media porosity occurred at Test Condition 5 of the field experiments, in triplicate, allowing a measurement of the media bed with a fully established biofilm present. Testing commenced approximately 4 to 6 hours after following backwashing of the unit to

minimize excess biomass buildup. The porosity of the media within the pilot-scale column was determined using manometry. A clear 13 mm I.D. flexible vinyl tube was attached to an influent sample line located below the pilot unit underdrain. The tube ran vertically along the height of the column and was open to the atmosphere at the top end. The column was prepared for porosity testing by 1) stopping aeration 2) draining water from the column to a height slightly above the media/support gravel interface to dispel any stagnant bubbles remaining within the media, and 3) slowly pumping influent into the column again in an upflow manner. Steps 2 and 3 were repeated twice. Finally, the column was filled to approximately midway and the ball valve on the manometer was opened. Water in the column and manometer was allowed to settle for approximately 10 minutes, and the initial height of water in the manometer was recorded. A visual inspection showed that 10 minutes was sufficient to allow the water level in the manometer to come to a stable height. An approximately known volume of water (42.50 L) was then pulled from the 6.4 mm influent sample port at the bottom of the reactor. The remaining water in the column was then allowed to settle for approximately 10 minutes and a final height of the manometer was recorded.

Endogenous respiration

For a period of 1 hour ($\geq$ 3 HRTs) prior to testing, aeration was stopped and no supplemental feed was provided to the unit. The superficial liquid velocity remained at the process conditions. Bulk dissolved oxygen concentrations were sampled and recorded after the hour waiting period at each of the six sampling sites (influent, Ports 1 through 4, and effluent) using sampling protocols identical to those used for the aeration testing. Grab influent and effluent samples (500 mL each) were collected and stored in a cooler for transport. The samples were analyzed for the standard parameters as summarized in Table 2.2. DO profiles were collected during Test Condition 3 after 23 and 51 hours of normal run time, and Test Condition 4 after 25 and 49 hours of normal run time.

Biological observed yield

Samples were collected from the effluent weir of the pilot unit during the backwash sequence between the time when the water level initially reached the weir and the conclusion of the

final rinse steps (approximately 24 minutes). A series of 49 individual 250 mL grab samples were taken in 30 second intervals to form a composite sample. A 1 L representative sample was collected, stored in a cooler for transport to the laboratory, and analyzed according to the parameters as outlined in Table 2.2. Samples were analyzed in triplicate, as a minimum. Composite influent and effluent samples were collected (500 mL each) over the course of the previous filter run cycle with the refrigerated sampler system. Samples were stored in a cooler for transport to the laboratory and analyzed for parameters as summarized in Table 2.2. The test was performed in duplicate under Test Condition 5 after 24 hours and 48 hours of filter run time, respectively.

RESULTS AND DISCUSSION

Minimum aeration requirement testing

The BAF pilot unit achieved full ammonia removal within 6 weeks of starting operation. The unit was then operated for two additional weeks to establish stable ammonia oxidation before aeration testing was started. During startup, effluent nitrite levels reached 0.9 kg $N/m^3/d$ on day 29 of startup but had consistently dropped to negligible concentrations during weeks 6 to 8. Meanwhile, a general increase in effluent nitrate levels observed during startup showed that nitrate was effectively generated within the column. Following startup of the unit, no significant nitrite accumulation (> 0.2 kg $N/m^3/d$) was observed at any of the profile ports with the exception of during the first Test Condition. During the first week of testing, nitrite levels were measured by ion chromatography but were artificially inflated due to interference from high chloride levels present in the sample matrix. Subsequently, the nitrite determination method was revised to a colorimetric method. Table 2.3 shows that the pilot unit maintained sufficient growth conditions for nitrification during all Test Conditions, suggesting that dissolved oxygen was the changing variable that limited growth. Overall, the bulk DO concentrations entering the pilot were close to saturation and decreased with increased nitrifier activity. In general, minimum DO levels were observed between Sampling Ports 1 and 3, the area of greatest respiration activity. DO levels then increased again towards the top of the media bed. The DO sag profile became more significant within the column with decreasing aeration rates, although the DO never fell below the typical oxygen half-saturation constant for autotrophic bacteria of 0.75 mg/L O_2, (Grady et al. 1999).

Table 2.3: BAF loading and performance during testing conditions. Error values represent one standard deviation value from each day of testing.

	Testing Condition				
Parameter	**1**	**2**	**3**	**4**	**5**
Water Temperature (^oC)	24.2 ± .6	21.1 ± .9	19.1 ± .6	18.1 ± .2	15.5 ± .9
$pH_{initial}$	8.60 ± .14	8.06 ± .16	8.54 ± .17	8.60 ± .07	8.72 ± .14
pH_{final}	6.93 ± .12	6.72 ± .19	6.78 ± .12	6.71 ± .05	6.99 ± .13
$Alkalinity_{initial}$ (mg/L as $CaCO_3$)	381 ± 10	176 ± 7	294 ± 22	184 ± 16	456 ± 40
$Alkalinity_{final}$ (mg/L as $CaCO_3$)	96 ± 24	87 ± 6	79 ± 14	78 ± 9	165 ± 56
NH_4-N Unit Loading Rate ($kg/m^3/day$)	1.1 ± 0.1	1.4 ± .09	1.5 ± .03	1.1 ± .13	1.5 ± .14
NH_4-N Media Bed Loading Rate ($kg/m^3/day$)	0.9 ± 0.09	1.3 ± .08	1.4 ± .03	1.0 ± .11	1.4 ± .17

Figure 2.2 shows the remaining ammonium-N load as a function of the column height for each of the five Testing Conditions. Complete ammonium oxidation was verified at each Test Condition by monitoring the concentration profiles for each of the inorganic nitrogen species (not shown). The dotted ammonium-N loading line on each plot represents the targeted maximum effluent level for each Condition. The desired pilot unit ammonium removal capability of each of the testing conditions was attained within days of a change in loading. Figure 2.3 shows a comparison between the theoretically determined aeration rates required for the desired ammonium load removal and the corresponding achievement for the aeration rates tested.

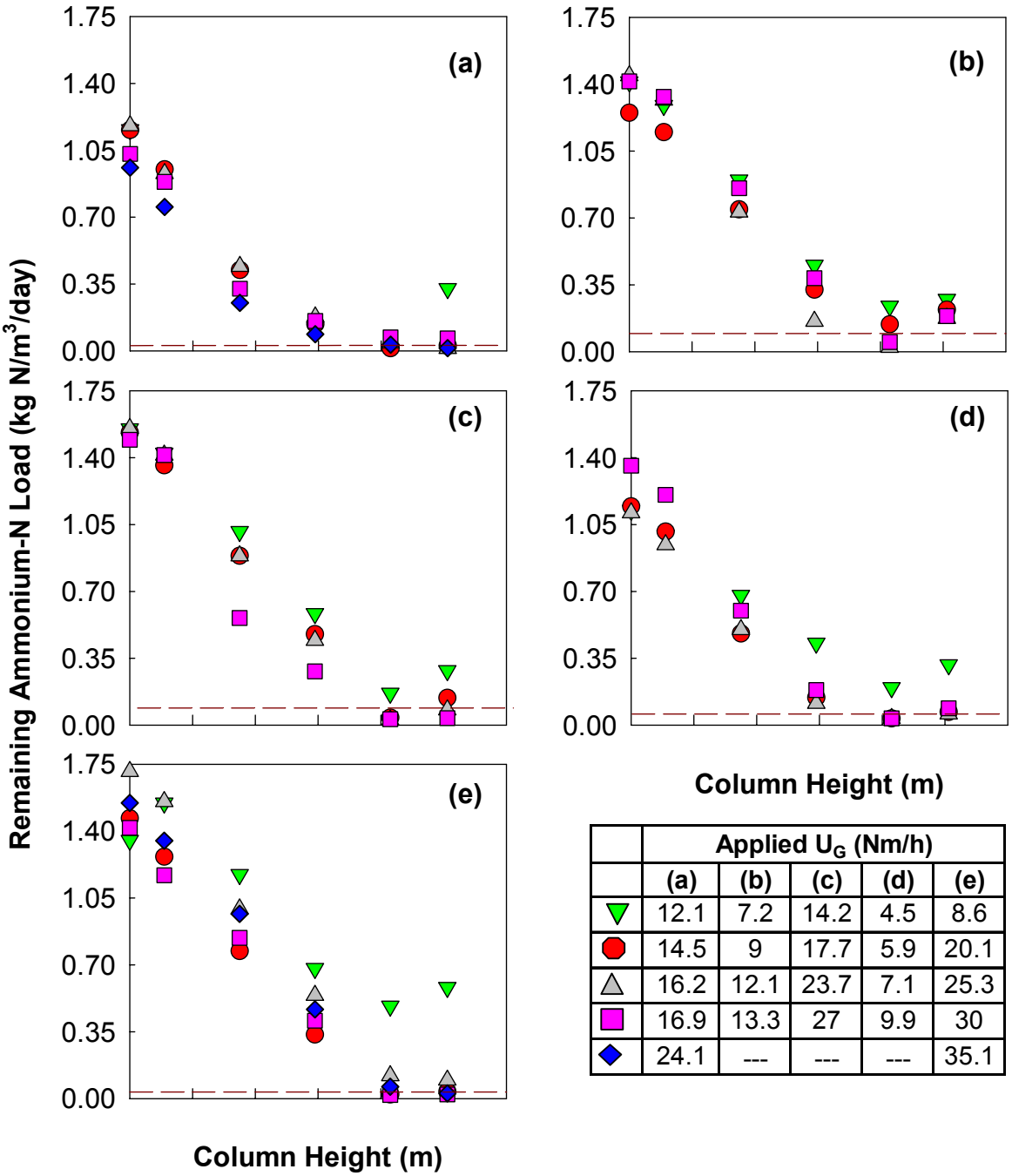

	Applied U_G (Nm/h)				
	(a)	(b)	(c)	(d)	(e)
▽	12.1	7.2	14.2	4.5	8.6
○	14.5	9	17.7	5.9	20.1
△	16.2	12.1	23.7	7.1	25.3
□	16.9	13.3	27	9.9	30
◇	24.1	---	---	---	35.1

Figure 2.2: Remaining concentrations of ammonium-nitrogen at various applied superficial air velocities for applied N loadings of (a) Testing Condition 1 (b) Testing Condition 2 (c) Testing Condition 3 (d) Testing Condition 4 (e) Testing Condition 5

All aeration rates tested during Test Condition 1 exceeded the theoretically determined demand although the desired ammonium-N load was not removed at aeration rates of 12.1 and 16.9 Nm/h. High nitrite peaks (up to 0.4 kg N/m^3/d) were observed within the media bed during each day of testing with accumulations concentrated at the base of the media bed.

The nitrite levels were then oxidized to nitrate as the wastewater traveled up the media bed with low concentrations found in the pilot effluent. At an aeration rate of 12.1 Nm/h, the resulting lowered ammonium-N removal capacity can be explained by mechanical difficulties with the unit. At an aeration rate of 16.9 Nm/h, the lowered ammonium-N removal capacity may have been a result of sampling the Test Condition only 5 hours following a backwash due to scheduling constraints.

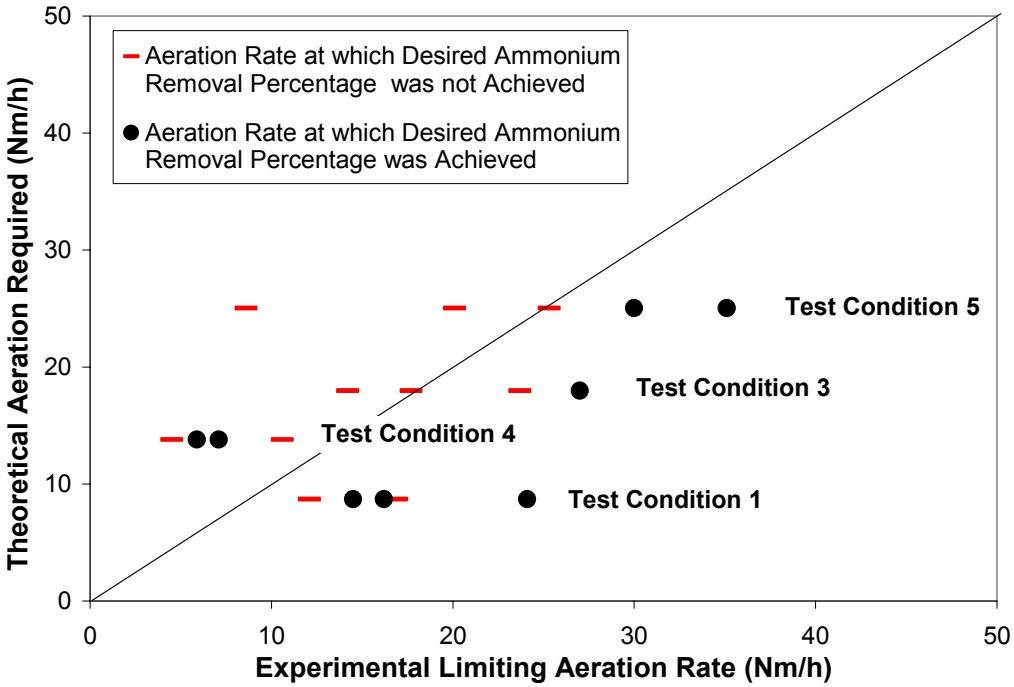

Figure 2.3: A comparison of the experimentally determined limiting aeration rate vs. the theoretically determined aeration requirement for a given Test Condition.

As the pilot unit stabilized for testing at Test Condition 2, the unit began to experience progressive bed clogging due to repeated insufficient backwashing conditions. Evidence of clogging was evident based on the increasing differential pressure within the media bed despite backwashing. Although partial nitrification continued to be achieved throughout the week of testing, the unit was not able to meet the targeted effluent ammonium-N level at any aeration rate tested. In addition, a slight increase in media bed height was observed, which may have been due to the presence of clumped media sections caused by "dead" aeration zones. A decreased volume of media would therefore be available for nitrification to occur.

Therefore, the data obtained from the second test condition was not analyzed further since it would not be representative of the characteristics of a fully functioning unit.

At Test Condition 3, the effluent ammonium loading was not achieved at aeration rates of 14.2, 17.7, and 23.7 Nm/h. Nitrite concentrations within the media bed remained low (< 0.07 kg NO_2-N/m^3/day) over the height of the column bed as effluent nitrate concentrations increased for the range of aeration rates tested. During Test Condition 4, all aeration testing conditions were below the theoretically determined aeration requirement although the pilot unit achieved the required ammonium removal loading at aeration rates of 5.9 and 7.1 Nm/h. Low nitrite concentrations (< 0.05 kg NO_2-N/m^3/day) were observed for all the testing conditions, peaking at the base of the media bed and decreasing as the wastewater rose through the column. At Test Condition 5, the desired load reduction in the effluent was achieved at aeration rates exceeding that theoretically required (30 and 35.1 Nm/h). Nitrite concentrations within the media bed remained extremely low (< 0.007 kg NO_2-N/m^3/day) over the height of the column bed for the range of aeration rates tested with the highest concentrations observed at the base of the media bed.

Results from the aeration testing indicate that at higher pollutant loading rates, the aeration required by the pilot was approximately equal to or slightly lower than the rate determined stoichiometrically despite assuming the large OTE factor of 20%. Although the theoretically determined requirement was exceeded at an aeration rate of 23.7 Nm/h during Test Condition 3, the unit failed to meet the desired effluent loading by less than 0.03 kg NH_4-N/m^3/day or 0.6 mg/L. Meanwhile, the unit may have been unable to meet the desired effluent loading at an aeration rate of 25.3 Nm/h during Testing Condition 5 due to a 0.2 kg NH_4-N/m^3/day increase in loading from the previous day of testing rather than an oxygen limitation. At lower pollutant loadings of 1 kg NH_4-N/m^3 of media/day, the theoretical aeration requirement most likely resulted in overaerating the unit. The unit was able to achieve the nitrification capacity requirement using as low as only 50% of that required stoichiometrically as observed during Test Condition 4. In addition, higher hydraulic rates did not seem to retard effective and efficient transfer of oxygen to the liquid phase for the water ranges tested. Whereas the typical OTE factors for activated sludge are between 6 to

15% (Grady et al., 1999), the results from the aeration testing suggest that the BAF pilot unit has an OTE factor slightly higher than the previously assumed value of 20%.

As a fully nitrifying column, the media bed within the pilot-scale unit was able to successfully handle the highest hydraulic loadings tested of up to 10.4 m/h and pollutant media loading rates up to 1.4 kg NH_4-N/m^3/day. A comparison between Test Conditions show that similar ammonium loadings result in analogous linear ammonium removal rates despite different hydraulic loadings and initial ammonium concentrations. As expected, most ammonium removal occurred at the base of the unit and minor concentrations of ammonium were removed in the upper section of the media bed at the lower pollutant loadings (Test Condition 1 and 4). Overall, each set of testing conditions show a clear trend that when other environmental factors are not limiting, there is a distinct positive correlation between the ammonium removal load and the aeration rate (Figure 2.4). Conditions in which the unit experienced excessive aeration are not shown for the remaining figures. Excessive aeration has been defined by the authors as a situation where the difference between the DO levels in the bulk influent and the minimum DO measured within the column bed is less than 1.5 mg/L. The criteria eliminated aeration rates of 16.9 and 24.1 Nm/h during Test Condition 1 and aeration rates of 30 and 35.1 during Test Condition 5.

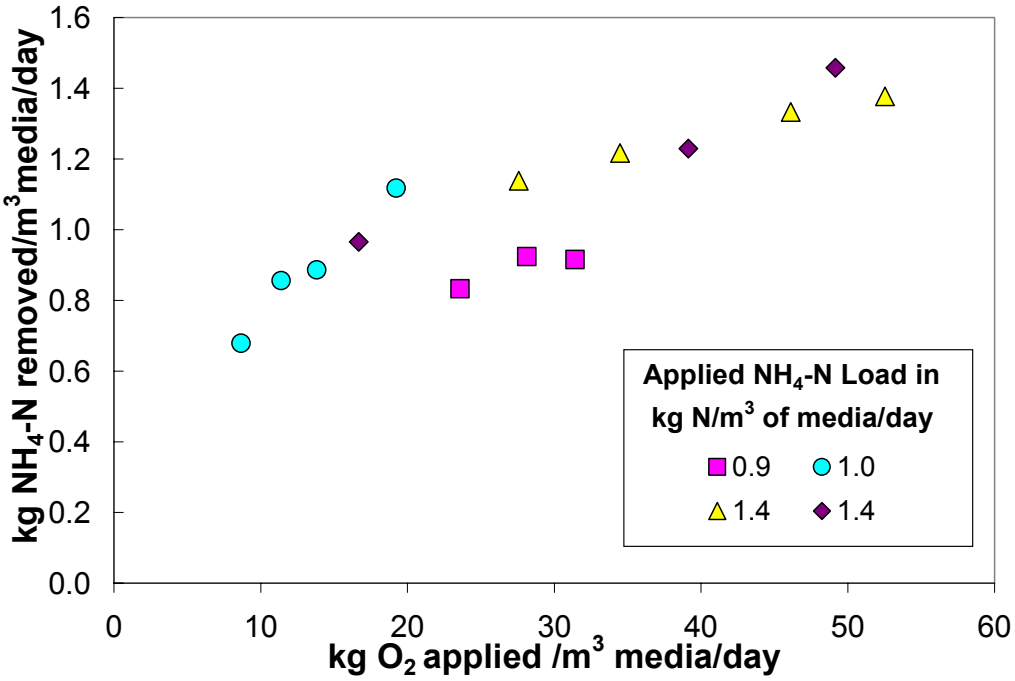

Figure 2.4: The removal of ammonium-N based on an applied oxygen loading for a given applied ammonium loading for Test Condition 1(□), Test Condition 3 (Δ), Test Condition 4 (O), and Test Condition 5 (◊)

Biological yield

The observed biomass yield determination experiments were performed approximately two weeks apart at Testing Condition 5. Aeration was not a limiting factor during yield testing. Composite influent ammonium-N concentrations were 35.2 mg/L and 38.7 mg/L during the 24 and 48 hour filter runs, respectively and observed yield was calculated using Equation (2.12).

The observed yield was determined to be 0.24 and 0.14 mg COD as cell generated per mg NH_4-N removed for the 24 and 48 hour filtration runs, respectively. Both yield determinations are within the range typically found for nitrifiers (Grady et al., 1999). A lower yield was determined after a 48 hour filter cycle, and can be explained by the impact of decay on the observed yield. Over 48 hours, a greater extent of decay occurs relative to a 24 hour run and is reflected in less net biomass remaining. The low nitrifier yield in a tertiary system allows the system to continuously filter for the standard 48 hours without significantly increasing the bed headloss by clogging the filter bed. Since testing occurred on

the pilot unit using 48 hour filtration runs, an observed yield value of 0.14 mg COD as cell generated per mg NH_4-N removed was used for all calculations.

Endogenous respiration

A series of endogenous respiration tests was performed on the column to determine the degree of oxygen demand the decay material had on the overall respiration rate and to observe the distribution of biological respiration along the column bed. Endogenous respiration can serve as a measure of the active bacteria within the column. The input of unsupplemented secondary effluent into the unit for several hydraulic retention times prior to testing insured that both the inlet and effluent process water possessed the similar chemical characteristics. Without an external electron donor, the only source of energy for active cells was other cellular tissue (Tchobanoglous et al., 2003). Overall, the endogenous respiration requirement for the BAF unit ranged from 2 to 7% of the total respiration demand.

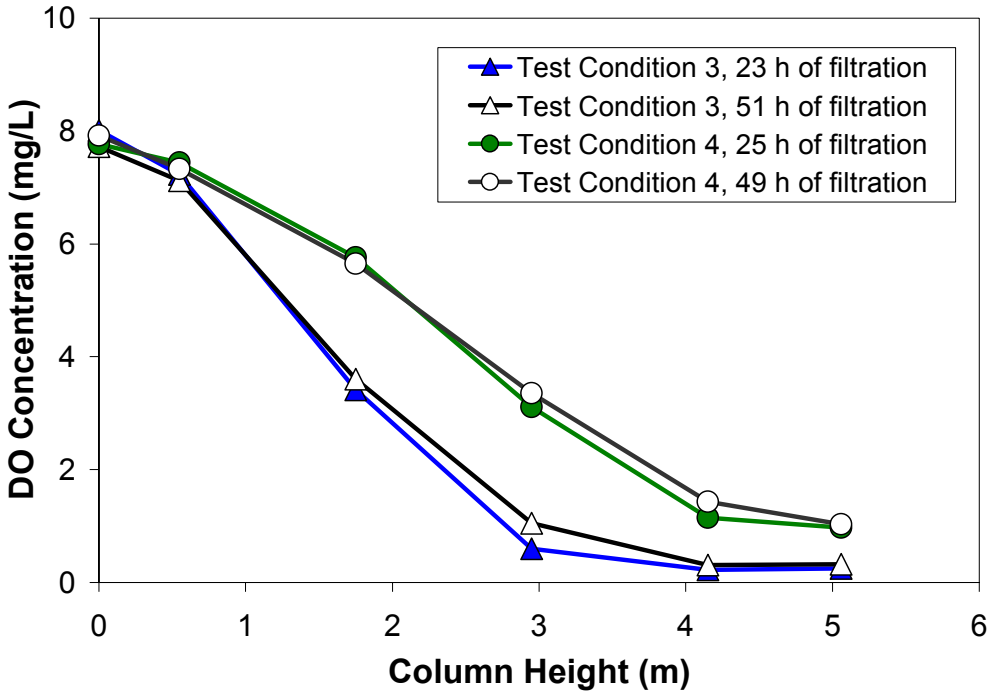

Figure 2.5: Endogenous respiration vs. column height at Test Condition 3 (U_L=7.4 m/h, 1.4 kg NH_4-N/m^3 media/day) and 4 (U_L=10.4 m/h, 1.0 kg NH_4-N/m^3 media/day) after 24 and 48 hour filter runs, respectively.

Figure 2.5 shows the mass of dissolved oxygen consumed between each of the sampling ports for four separate experiments. From the figure, it is evident that there is no significant

difference between the quantity of active bacteria after approximately 24 hours of filtration or 48 hours of filtration. Rather, it can be shown that the established location and degree of endogenous respiration changes as a function of the hydraulic and pollutant loads. At the lower hydraulic loading but higher pollutant loading (Test Condition 3), the bacterial respiration is concentrated between Ports 1 and 3. The condition results in a high concentration of bacteria distributed closer to the inlet of the unit. At the higher hydraulic loading and lower pollutant loading (Test Condition 4), the unit experiences a more distributed active respiration rate over the column bed.

K_La determination

The experimentally measured chemical analysis and DO profiles across the pilot unit provided the basis for determining the oxygen mass transfer coefficients for each series of Test Conditions. The estimated pilot scale BAF porosity (0.297 ± 0.02) matched closely with that measured in the bench scale abiotic BAF unit in the preceding chapter (0.293 ± 0.03). Using Equation (2.7), individual K_La values for the 1) combined gravel support layer, 2) media layer between Port 1 and 2, 3) between Port 2 and 3, 4) between Port 3 and 4, and 5) overall 2.7 mm media bed were approximated. The calculated K_La values across the combined gravel layer tended not to follow any distinct trends and resulted in scattered values ranging from 27 to 99 h^{-1}. Two separate methods were utilized to determine the observed K_La factor across the 2.7 mm media bed. The first method averaged the three individual K_La values determined across each of the two adjacent media bed ports (e.g. Ports 1 and 2) and is hereafter referred to as the Port method of determining oxygen mass transfer within the pilot. The second method approximated a single K_La value determined across the entire 2.7 mm media bed and is hereafter referred to as the Overall method. The Port method resulted in K_La values ranging from 64 to 158 h^{-1} for the range of conditions tested whereas the Overall method resulted in K_La values ranging from 56 to 167 h^{-1}. Repeatability of the test profiles was observed at Test Condition 4 and superficial air velocity of 5.9 Nm/h. The series of liquid sample and dissolved oxygen profiles were collected approximately 3 hours apart with a 0.14 kg NH_4-N/m^3/day increase in the influent between test duplicate 1 and 2. For the duplicates, the average media bed K_La determination based on the Port method resulted in values of 87 and 117 h^{-1}. The resulting overall K_La values based on the Overall

method of calculation were 85 and 122 h^{-1}. Although the Port method seemed to provide a more precise estimate of mass transfer values, the two calculation methods provided similar results. Since Equation (2.7) calculates an averaged approximation of oxygen transfer over a finite height within the media bed, similar results between the 2 calculation methods imply that the overall biological respiration rate (r_N - r_G +r_E) plays the major role in determining the rate of oxygen transfer into liquid phase under non-limiting environmental conditions.

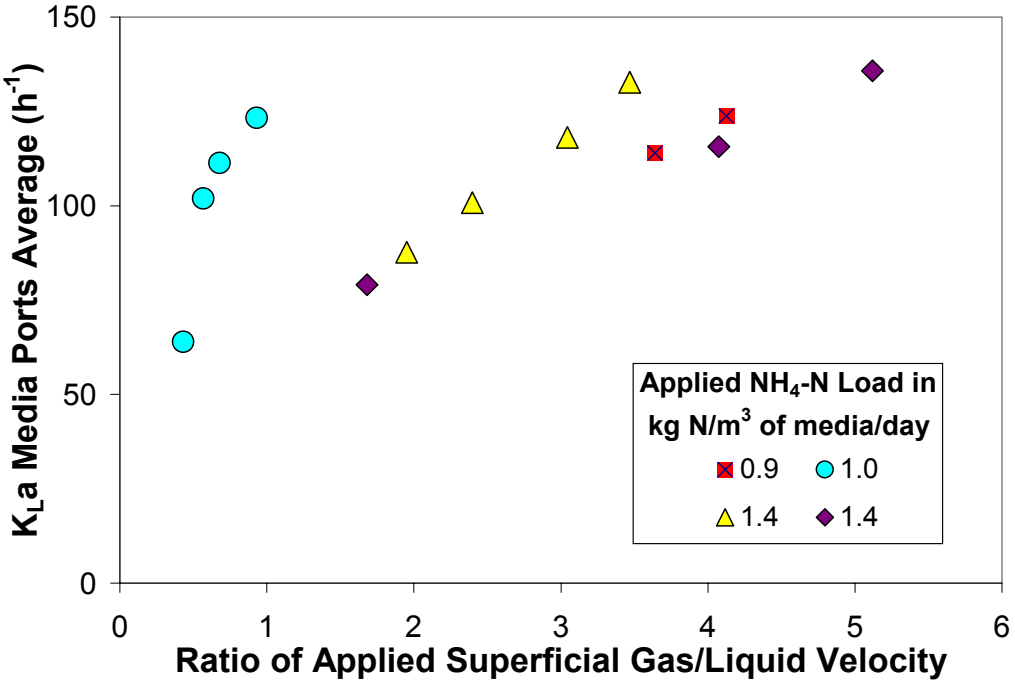

Figure 2.6: Superficial gas/liquid velocity ratio vs. experimentally determined K_La using the Port method for the applied media bed nitrogen loadings.

A more in-depth comparison can be made regarding approximating the K_La values across the 2.7 mm media bed. Figure 2.6 shows the K_La values as calculated using the Port method. Overall, the oxygen transfer values follow an increasing trend as the ratio of applied superficial gas velocity to the superficial liquid velocity increases. In addition, a distinct increasing trend is also observed for most of the individual testing conditions.

Oxygen transfer enhancement

A comparison between the predicted K_La value determined by the abiotic testing (Leung et al., 2003) and the experimentally determined K_La values calculated in the biologically active

system was made by determining the associated transfer enhancement factor with the following equation:

$$K_L a \text{ Enhancement Factor} = \frac{\text{biotic experimental } K_L a}{\text{abiotic predicted } K_L a} \quad (2.17)$$

The abiotic $K_L a$ factor for the media was determined previously to be (Leung et al., 2003):

$$K_L a_{(T)}(\text{wastewater}) = (\alpha) \cdot (c) \cdot U_G^a \cdot U_L^b \cdot \theta^{(T-20)} \quad (2.18)$$

where the terms of α, c, a, b, and θ are previously correlated empirical factors specifically for the 2.7 mm media. It should be noted that the α factor was assumed to be 0.7 which was previously determined for the wastewater of another domestic wastewater treatment plant. Figure 2.7 shows a consistent presence of a slight transfer enhancement, in support of the hypothesis that a transfer enhancement occurs within the media beds containing biomass. The enhancement factor hovers between approximately 1.1 and 1.7. A similar comparison was made regarding the support gravel but the scatter in the data was significant and the results did not support the enhancement factor theory for the range of gas and liquid velocities tested (data not shown). The scatter of the data for the gravel is assumed to be due to the close proximity of the air diffusers to the gravel layer which may cause disturbances and decrease the reproducibility of the $K_L a$ estimates values.

The presence and packing structure of the 2.7 mm media may be the cause of the oxygen transfer enhancement which occurs when the gas bubbles rise through the pilot-scale unit. A visual inspection of the gas bubbles traveling through the gravel beds in a bench-scale unit (Leung, 2003) showed that the somewhat large void areas between the gravel particles allowed the bubbles to retain their original shape. Despite a relatively high porosity stemming from internal grain pores, the structure and shape of packed 2.7 mm media provide little external pore space between the grains. Hence, the gas bubbles are forced to elongate to gain passage through the column. It is hypothesized that bubble elongation along with a strong oxygen demand from respiring nitrifiers significantly influences the dynamics of the oxygen mass transfer in the BAF pilot tested.

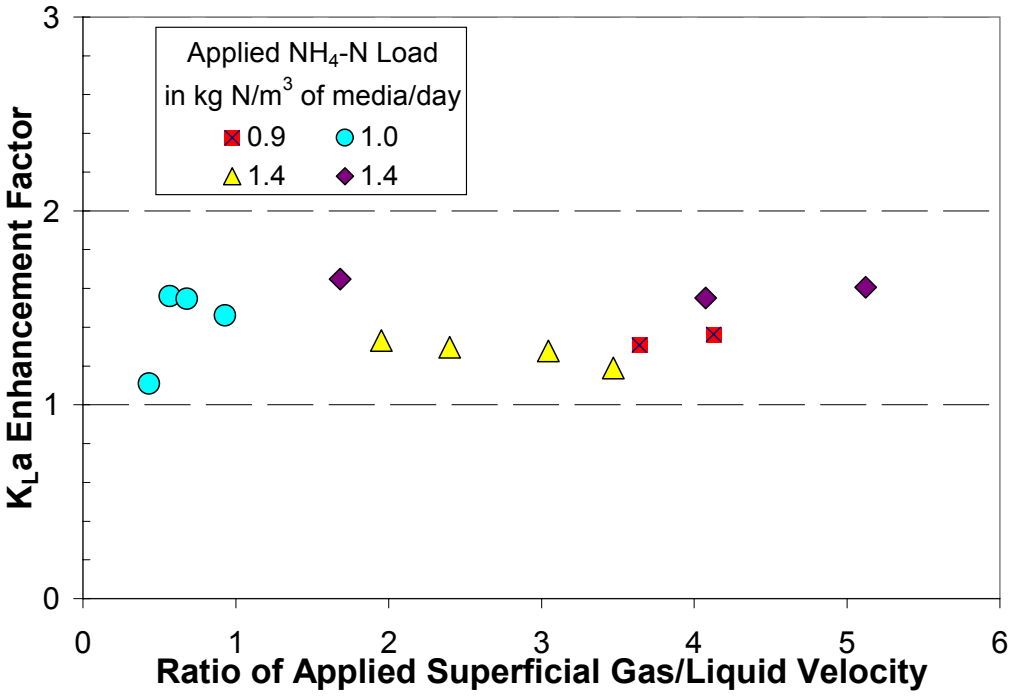

Figure 2.7: The ratio of gas to liquid velocity vs. enhancement factor in 2.7 media using the K_La – Port method for the applied media bed nitrogen loadings.

Bubble enhancement theory

It is postulated that the enhancement oxygen transfer factor found in the media bed may be attributed to both the densely populated bacterial population producing a high biological demand per given volume and the available void space within the media bed. Oxygen flux is a function of both the K_La factor and the driving force, as shown in Equation (2.19). Hence, the flux can be biologically enhanced if the bacteria can either influence the K_La value (as shown previously) or the DO driving force (C_{sat}-C). As a highly oxygen intensive process, nitrification requires that oxygen must constantly be transferred from the air bubbles to the established biofilm through the water. The constant oxygen demand establishes a dissolved oxygen gradient in the thin boundary layer between the gas bubble and the oxygen intensive biomass (C_{BL}) and bulk (C_{bulk}) water layers. Such a gradient would not be present within the media bed under abiotic conditions for either clean water or wastewater due to the absence of oxygen consuming sites. The presence of the gradient can be significant in areas of high oxygen demand since it serves to increase the flux of oxygen: $(C_{sat} - C_{bulk}) << (C_{sat} - C_{BL})$. If such a condition were present, it would provide a theoretical basis for calculating a higher

oxygen mass transfer factor in the biologically active system than in an identical abiotic system due to an enhanced driving force. In essence, the bulk phase DO measurement underestimates the effective DO concentration that drives the flux of oxygen in biologically active regions.

$$J = K_L a \left(C_{sat} - C_{bulk} \right) \tag{2.19}$$

The significance of the impact of a dissolved oxygen gradient in the boundary water layer between the gas bubble and the biomass can be shown by determining the fractional increase in the driving force required within the 2.7 mm media bed to account for the presence of the biological enhancement of oxygen transfer. Microsoft Excel XP's Solver program was utilized to estimate the "effective" dissolved oxygen concentrations in the boundary layer liquid (C_{BL}) for the pilot unit at each media port while the setting the $K_L a$ enhancement factor (Equation (2.17)) to 1.0. For this analysis, it is assumed that the DO concentration gradient drives the enhanced oxygen flux rather than a difference in $K_L a$ between biotic and abiotic environments. In order to assume the nitrifiers were not oxygen-starved within the media bed and affecting biological kinetics, the solved DO values in the boundary layer were constrained to be equal to or greater than the oxygen half-saturation constant for autotrophic bacteria of 0.75 mg/L (Grady et al, 2003).

As shown in Figure 2.8, correlating trends can be established between the aeration rates and the relative boundary layer versus bulk layer-controlled driving force for oxygen transfer. In general, it can be shown that if a dissolved oxygen gradient is present between the bulk water and the boundary layer liquid, the resulting increase in the driving force ($C_{sat} - C_{bulk} < C_{sat} - C_{BL}$) can account for the enhanced oxygen transfer in dense media based biological aerated filters. The enhancement factor was not noticeable for aeration rates in significant excess or lower than that required stoichiometrically as summarized in Table 2.1. In those cases, the dissolved oxygen gradient may be small and the oxygen transfer is dictated almost exclusively by the traditional diffusion oxygen transfer kinetics.

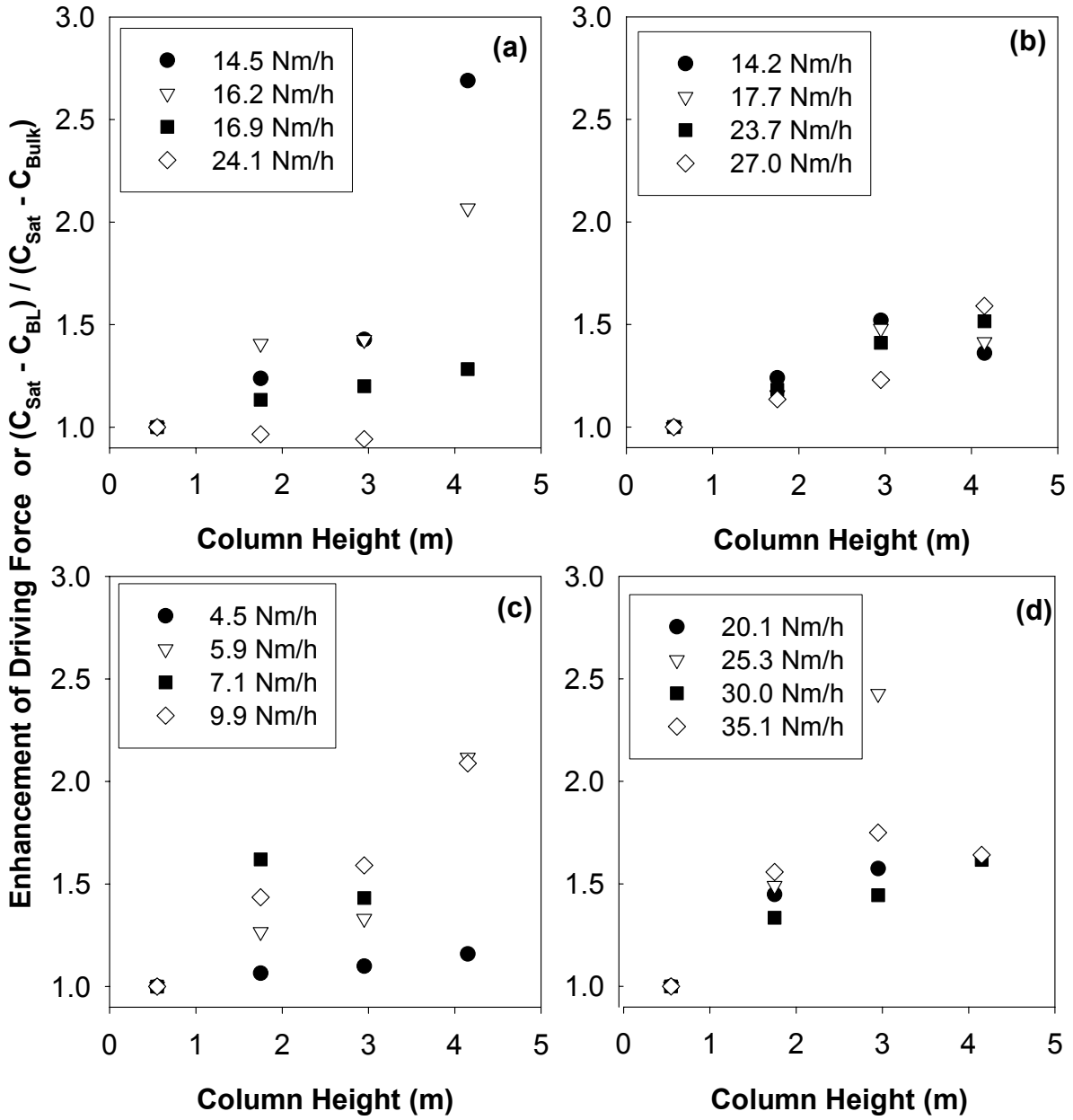

Figure 2.8: The fractional increase in the driving force within the 2.7 mm media bed for each aeration rate to account for the presence of an enhancement factor for applied ammonium-N loadings of (a) 0.9 kg/m^3 media/day (b) 1.5 kg/m^3 media/day (c) 1.1 kg/m^3 media/day (d) 1.5 kg/m^3 media/day.

In order to support the large respiration demands required for elimination of the pollutant load applied, the biomass establishes an environment closer to maximum oxygen transfer kinetics occurring between the bubble, liquid, and biomass layers than that measured in the bulk water. Higher transfer rates can be obtained in the presence of thinner boundary water layers between the oxygen gas and a source of high oxygen consumption like the biomass.

The nature of the packed media bed tested and unit backwashes provide an environment which minimizes the external void area between the grains for the air bubbles and process water to pass through. In addition, Delahaye et al. (1999) showed that a significant fraction of the biomass present in the interstitial void space of upflow carbonaceous and ammonium removal BAF units (25 to 40%) have physiological features closer to that of suspended cultures. Such conditions result in even smaller void spaces for bubbles to "squeeze" in the remaining space between the biofilm-coated media grains and the detachable biomass as the gas bubble travels up the column. The overall effect can result in thinner liquid boundary layers between the gas bubbles and both fractions of biomass than that in suspended culture systems.

The theory still requires that the oxygen demand from the biomass be greater than the oxygen transfer rate from gas to liquid for a dissolved oxygen gradient to exist within the media bed. For simplicity of calculations, it is assumed that all the biomass behave as a biofilm. The dissolved oxygen availability can then be calculated by dividing the average assumed dissolved oxygen concentration in the boundary water layer by the transfer time available between a given bubble and the associated boundary layer, which is conservatively assumed to be two-thirds the contact time between the boundary layer and the bubble (see Equation (2.20)). The dissolved oxygen demand can be calculated by multiplying the biomass surface area directly in contact with the elongated cylindrical bubble with the biomass oxygen consumption rate based on the media surface area available (see Equation (2.21)). The ratio of the oxygen demand from the biomass versus its availability in the boundary water layer can then be calculated with the parameter assumptions shown in Table 2.4 and the following equations:

$$DO\ Available = \frac{C_{BL} \times \left[\pi \left(b_{CL} \times 2L_T \right) \left(\frac{b_{CD} + 2L_T}{2} \right)^2 - \pi \left(b_{CL} \right) \left(\frac{b_{CD}}{2} \right)^2 \right]}{\frac{2b_{CL}}{3V_b}} \tag{2.20}$$

$$DO\ Demand = 2\pi (b_{CL}) \left(\frac{b_{CD}}{2} \right)^2 \times r_{bio} \times m_{SA} \tag{2.21}$$

Since the theory contends that the oxygen concentration present within the boundary layer must be lower than the concentration found within the bulk water, the boundary layer oxygen concentration was chosen as the system variable. The ratio of oxygen demand versus the mass of oxygen available can then be compared between the assumed dissolved oxygen in the boundary layer available and parameter estimates.

Results indicate that the demand is smaller than the available amount only at high average DO concentrations (> 6 mg/L) in the boundary layer and either small biomass surface areas adjacent to the boundary layer or a thick boundary layer thickness. The ratio dictates that a dissolved oxygen gradient would be not present between the bulk liquid and the boundary layer liquid if the average air bubble diameter was greater than 5 mm or the thickness of the boundary layer between the bubble and the biofilm equaled or exceeded 2 mm. Otherwise, a dissolved oxygen gradient would be present between the bulk liquid and the boundary layer liquid for the full range of elongated bubble diameters, bubble rise velocities, and biological oxygen consumption rates tested.

Parameter sensitivity

A parameter sensitivity analysis can be performed to test the relative influence of the approximated parameters involved in made for the bubble enhancement theory. The analysis will give an indication of the significance of the parameter estimates. Each of the five parameters was tested against the range of initial dissolved oxygen concentrations in the boundary layer water from 0 to 8 mg/L parameter for its relative sensitivity in the proposed bubble enhancement theory. The relative sensitivity of the five parameters was run for the same range of values anticipated to be present within the column as indicated in Table 2.4. Relative sensitivity was determined in Equation (2.22) as defined by Saltelli et al. (2002). Significant sensitivity was then defined at a relative sensitivity level of 10 or greater

$$S_R = \frac{(O - O_{BL})PA_{BL}}{(PA - PA_{BL})O_{BL}} \tag{2.22}$$

It was found that only 14 of the 150 scenarios tested resulted in significant relative sensitivity or that did not support the theory that the biomass oxygen demand was greater than the amount available in the boundary layer. Parameters b_{SD} and r_{BIO} were found to have high significance at initial DO concentrations of 0, 6, and 8 mg/L in the boundary water layer for the parameter estimates closest to the baseline values. Parameters b_{CD} and L_T were found to have high significance only at the highest DO concentrations tested. Of those, the two most critical parameter estimates made were the original gas bubble diameter and the biological oxygen consumption rate. The bubble rise velocity, or the contact time between the air and the boundary water, was not found to have significant sensitivity impact at any DO concentration. It was therefore concluded that the enhanced bubble theory postulated could roughly account for the enhanced oxygen transfer rate occurring within the biologically active BAF unit.

Table 2.4: Parameter estimates for the bubble enhancement theory

Parameter Description	Symbol	Parameter Range Tested	Baseline Assumption	Units
(1) Initial bubble diameter	b_{SD}	0.5 – 1.2	0.75	cm
(2) Characteristic elongated "cylindrical" diameter	b_{CD}	0.0001 – 0.005	0.0025	m
(3) Bubble rise velocity	V_b	15 – 40	25	cm/s
(4) Water film thickness in boundary layer	L_T	0.0005 – 0.002	0.001	m
(5) Initial oxygen concentration in boundary layer	C_{BL}	0.0 – 8.0	3	g/m^3
(6) Biomass oxygen consumption rate	r_{bio}	0.1 – 0.25	0.10	g/m^3s

CONCLUSIONS

1. It cannot be definitively concluded that the observed oxygen transfer factor is either due to biological activity or not simply an artifact of measurement/analysis techniques. Oxygen transfer measurement techniques continue to be contested, especially on larger scale units. Rather, the study looks at the resulting transfer values observed based on current measurement techniques.
2. Assuming an OTE factor of 20%, aerating the BAF pilot unit based on the stoichiometric aeration demand results in overaeration of the unit, especially at lower pollutant loading rates.

3. Endogenous respiration only accounted for 2 to 7% of the total oxygen requirement implying that the scheduled backwashes keep the majority of the biomass within the media bed highly active.
4. At higher pollutant loadings, bacterial respiration is concentrated closer to the inlet of the unit. At higher hydraulic but lower pollutant loadings, a lower, but more distributed, endogenous respiration rate is present over the column bed. This suggests that the regions of biomass activity change with loading conditions.
5. Overall, the oxygen transfer coefficient (K_La) in the 2.7 mm media bed increases as the ratio of applied superficial gas/ liquid velocity increases.
6. Rather than the enhancement resulting from a separate biological transfer pathway, it is postulated that the enhancement results from either an increase in K_La or the effective driving force. Based on a K_La increase, an enhanced oxygen transfer factor was determined in the biologically active pilot versus the abiotic testing (previous testing) to be between 1.1 to 1.7. Based on the intense oxygen demands present, the effective driving force $(C_{sat} - C_{BL})/(C_{sat} - C_{bulk})$ may be up to 2.7 times that observed.
7. It was postulated that the high biological oxygen demand and small void space force the air bubbles to "squeeze" in the remaining space between the biofilm-coated media grains and the detachable biomass as the gas bubble travels up the column. Under those conditions, it is more likely that a dissolved oxygen gradient is established in the reduced boundary layer thickness, forcing an enhancement in the oxygen transfer driving force between the gas and liquid phase.

ACKNOWLEDGEMENTS

Funding was provided by Degremont North American Research and Development Center, Inc. (DENARD) and Virginia's Center for Innovative Technology. We acknowledge the assistance of Julie Petruska and Jody Smiley of Virginia Tech as well as the personnel at DENARD in the successful completion of the experimental work. We would also like to acknowledge the Proctors Creek Wastewater Treatment Plant in Chesterfield, VA for their assistance and use of their facility.

REFERENCES

APHA-AWWA-WPCF. (1998). *Standard methods for the examination of water and wastewater*, 20th Ed., Washington DC.

Albertson, O. E. and DiGregorio, D. (1975). "Biologically mediated inconsistencies in aeration equipment performance." *J. Water Pollu. Control Fed*., **47**(5), 976-988.

Delahaye, A. P., Gilmore, K. R., Husowitz, K. J. , Love, N. G., Holst, T., and Novak, J. T. (1999). "Distribution and characteristics of biomass in pilot-scale upflow biological aerated filters treating domestic wastewater." *Proceedings of the IAWQ Conference on Biofilm Systems*., **10**, 17-20.

Franzini, J. B. and Finnemore, E. J. *Fluid Mechanics with Engineering Applications*. 1997. Boston, MA, McGraw-Hill. p. 142.

Fujie, K., Hu, H. Y., Ikeda, Y., and Kohei, U. (1992). "Gas-liquid oxygen transfer characteristics in an aerobic submerged biofilter for the wastewater treatment." *Chem. Eng. Sci.,* **47**(13-14), 3745-3752.

Grady, C. P. L., Daigger, G. T., and Lim, H. C. (1999). *Biological Wastewater Treatment*, Marcel Dekker, Inc., New York. p. 44, 199, 405, 415

Harris, S. L., Stephenson, T., and Pearce, P. (1996). "Aeration investigation of biological aerated filters using off-gas analysis." *Wat. Sci. Tech*., **34**(3-4), 307-314.

Iranpour, R., Magallanes, A., Zermeno, M., and Varsh, V. (2000). "Assessment of aeration basin performance efficiency: Sampling methods and tank coverage." *Wat. Res*., **34**(12), 3137-3152.

Jacob, J., Le Lann, J. M., Pingaud, H., and Capdeville, B. (1997). "A generalized approach for dynamic modeling and simulation of biofilters: application to waste-water denitrification." *Chemical Engineering Journal*, **65**, 133-143.

Ju, L. K. and Sundararajan, A. (1992). "Model analysis of biological oxygen transfer enhancement in surface-aerated bioreactors." *Biotechnology and Bioengineering*, **40**, 1343-1352.

Lee, K. M. and Stensel, H. D. (1986). "Aeration and substrate utilization in a sparged packed bed biofilm reactor." *J. Wat. Pollut. Control Fed*., **58**(11), 1066-1072.

Leung, S. M., Little, J. C., Holst, T., and Love, N. G. Mass-transfer characteristics of a biological aerated filter. 2003. *to be submitted for publication.*

LeTallec, X., Vidal, A., and Thornberg, D. (1999). "Upflow biological filter: Modeling and simulation of filtration." *Wat. Sci. Technol.,* **39**(4), 79-84.

Mann, A. T. and Stephenson, T. (1997). "Modeling biological aerated filters for wastewater treatment." *Wat. Res.,* **31**(10), 2443-2448.

Mendoza-Espinosa, L. and Stephenson, T. (1999). "A review of biological aerated filters (BAFs) for wastewater treatment." *Env. Eng. Sci.,* **16**(3), 201-216.

Mines, R. O. and Sherrad, J. H. (1987). "Oxygen transfer studies in activated sludge." *J. Water Pollu. Control Fed.,* **59**, 19-24.

Mueller, J. S. and Stensel H.D. (1990). "Biologically enhanced oxygen transfer in the activated sludge process." *J. Wat. Pollut. Control Fed*., **62**(2), 193-203.

Nogueira, R., Lazarova, V., Manem, J., and Melo, L. F. (1998). "Influence of dissolved oxygen on the nitrification kinetics in a circulating bed biofilm reactor." *Bioprocess Engineering*, **19**, 441-449.

Pelkonen, M. (1990). "Upgrading oxygen transfer in the activated sludge process." *Wat. Sci. Tech*., **22**(7-8), 253-260.

Poughon, L., Dussap, C. G., and Gros, J. B. (1999). "Dynamic model of a nitrifying fixed bed column: Simulation of the biomass distribution of *Nitrosomonas* and *Nitrobacter* and of transient behavior of the column." *Bioprocess Engineering*, **20**, 209-221.

Reiber, S. and Stensel, D. (1985). "Biologically enhanced oxygen transfer in a fixed-film system." *J. Water Pollut. Control Fed*. **57**(2), 135-142.

Rittmann, B. E. and Manem, J. A. (1992). "Development and experimental evaluation of a steady-state, multispecies biofilm model." *Biotechnology and Bioengineering*, **39**, 914-922.

Saez, P. B. and Rittmann, B. E. (1988). "Improved pseudoanalytical solution for steady-state biofilm kinetics." *Biotechnology and Bioengineering*, **32**, 379-385.

Saltelli, A., Chan, K., and Scott, E. M. (2000). Sensitivity Analysis, John Wiley and Sons, New York.

San, A., Tanik, A., and Orhon, D. (1993). "Micro-scale modeling of substrate removal kinetics in multicomponent fixed-film systems." *Chem. Tech. Biotechnol*., **58**, 39-48.

Selleck, R. E., Marinas, B. J., and Diyamandoglu, V. (1988). "Sanitary Engineering and Environmental Health Research Laboratory." Rep. No. UCB/SEEHRL Report No. 88-3/1, University of California, Berkeley, CA.

Sundararajan, A. and Ju, L. K. (1995). "Biological oxygen transfer enhancement in wastewater treatment system." *Water Environment Research*, **67**(5), 848-854.

Tchobanoglous, G., Burton, F. L., and Stensel, H. D. (2003). *Wastewater Engineering: Treatment and Reuse.* Metcalf & Eddy. New York. p. 705, 1050-1051.

Thogersen, T. and Hansen, R. (2000). "Full scale parallel operation of a biological aerated filter (BAF) and activated sludge (AS) for nitrogen removal." *Water Sci. and Tech*., **41**(4-5), 159-168.

Tsao, G. T. (1968). "Simultaneous gas-liquid interfacial oxygen absorption and biochemical oxidation." *Biotechnology and Bioengineering*, **10**, 765-785.

Vaxelaire, J., Roche, N., and Prost, C. (1995). "Oxygen transfer in activated sludge surface-aerated process." *Environmental Technology*, **16**, 279-285.

Ydstebo, L., Johnson, R., and Bilstad, T. (2001). "Enhanced nitrification in biofilms by optimized oxygen addition." *Proceedings of the WEF 74th Annual Conference and Exposition*; Atlanta, GA.